https://ntrs.nasa.gov/search.jsp?R=19700003296 2020-03-12T04:40:24+00:00Z

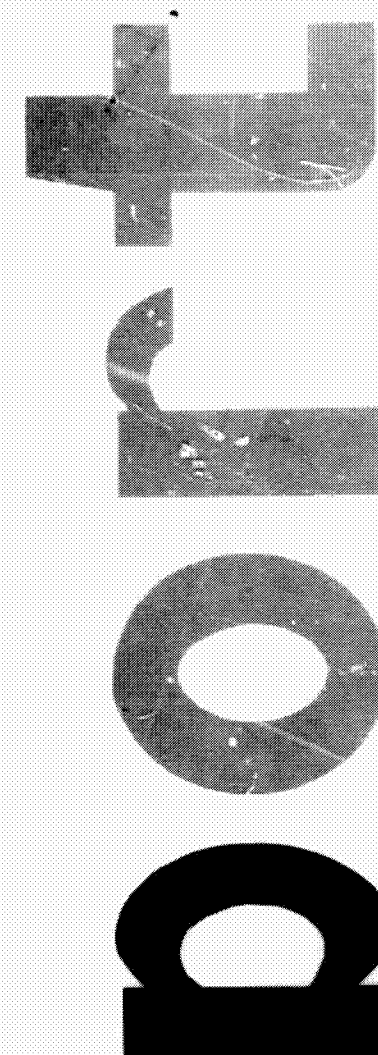

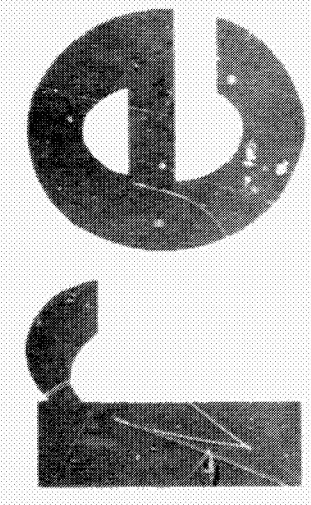

research

WYLE LABORATORIES
TESTING DIVISION, HUNTSVILLE FACILITY

FACILITY FORM 602

N70-12600
(ACCESSION NUMBER)
(THRU)
1
71
(PAGES)
(CODE)
CR 102370
(NASA CR OR TMX OR AD NUMBER)
28
(CATEGORY)

WYLE LABORATORIES - RESEARCH STAFF

REPORT WR 68-21

SPECTRAL TECHNIQUES IN JET NOISE THEORY

By

S.P. Pao and M.V. Lowson

Work Performed Under Contract NAS8-21060

April 1969

WYLE LABORATORIES
RESEARCH DIVISION, HUNTSVILLE FACILITY

COPY NO. 5

SUMMARY

Spectral analyses techniques are applied to Lighthill's aerodynamic sound equation to derive a unified jet noise theory, in which shear noise, self noise, and non-isentropic effects are treated on the same basis and derived simultaneously. The result of this theory has a simple, yet rigorous, representation of the radiated sound field.

The structure of the source terms in the turbulence and the mechanism of noise generation are examined in detail. Numerical examples of noise prediction are computed for two jet configurations where model turbulence structures are assumed. These examples demonstrate that this theory can predict correct sound pressure levels for a jet without any arbitrary constant.

TABLE OF CONTENTS

LIST OF TABLES AND FIGURES

LIST OF TABLES AND FIGURES (Continued)

LIST OF SYMBOLS

a	integral spatial scale of an isotropic turbulence
c_0	ambient speed of sound
c	local speed of sound in the turbulence; also abbreviation for c_0 .
c_p	specific heat at constant pressure
c_v	specific heat at constant volume
$E(k,\omega)$	scalar spectral function
$\underset{\sim}{F}$	applied force acting on the acoustic medium
G	general representation of the source function
h	total anthalpy
i	the imaginary unit
$i\ ,\ j$	indices
$\overset{M}{I}(\underset{\sim}{x},\omega)$	far field sound intensity
$\underset{\sim}{k}\ ,\underset{\sim}{\ell}$	wave numbers in cycles per unit length
M	convection Mach number
p	pressure
Q	mass flux
q	heat per unit volume
$\underset{\sim}{r}$	radial vector from the sound source to the observer
r_1, r	distance between the sound source and the observer
s_{ij}	constant mean flow shear gradient
t	time variable
T_{ij}	turbulence stress tensor

LIST OF SYMBOLS (Continued)

T	temperature, also time in limiting processes
$\overline{u}_0$	rms velocity fluctuation in the turbulence
u_i	fluctuating velocity component
U	mean flow velocity in the axial direction
v_i	velocity components
V	velocity, volume
$\underset{\sim}{x}$	position vector of the observer
$\underset{\sim}{y}$	position vector of the sour.
α	dimensionless ratio between the time and the spatial integral scales of the turbulence
β	integral time scale in the turbulence
γ	ratio of specific heat of a perfect gas
δ_{ij}	the Kronecker delta
θ	azimuth angle relative to the jet axis
$\underset{\sim}{\xi}$	a dummy spatial variable
ρ	density
τ	a time variable
$\phi(k,\omega)$	a one-dimensional spectral function
ω	frequency in cycles per second
ω_0	frequency in moving frame of reference
Λ	symbol for first order, or instantaneous spectrum
$\Lambda\Lambda$	symbol for second order spectrum
$\overline{}$	symbol for self-correlation function

$\sim$	symbol for vectors
r	subscript indicating component of a vectorial or tensorial quantity in the direction of the observer

1.0 INTRODUCTION

The advent of jet and rocket propulsion introduced a new form of noise, due to the high speed turbulent exhaust flows that characterize these engines. The noise from jet and rocket engines can cause both community noise and structural fatigue problems. In spite of considerable noise control effort jet engined aircraft are still a major source of noise intrusion in communities near airports. Rocket engine test schedules are also often controlled by potential community noise problems. Both aircraft and rocket vehicles have experienced fatigue failures in regions close to the engine due to the intense noise levels occurring near the exhaust. Thus there are many problems in jet and rocket noise which still require solution.

The problems are complicated by several factors. Although the noise field is clearly related in some way to the turbulence a wide variety of fluctuating mechanisms can be postulated as possible fundamental causes. Controversy still exists over whether the supersonic or subsonic portions of an exhaust flow are responsible for the major part of the noise. In some circumstances noise generated within the engine can be important while in others noise radiated far downstream due to instability mechanisms could be significant. At the present time the real contribution of either of these sources in a full scale case is unknown. Noise due to combustion, or even the effects of mean jet temperature are still essentially undetermined. Conflicting evidence is available regarding the possible significance of shocks in supersonic flow. Even such an apparently straightforward case as coaxial jet mixing has been found to cause almost insuperable problems in prediction by current techniques. Thus it appears that new methods are required.

The major part of the published theoretical work on exhaust noise has attempted to calculate the noise field by evaluation of the appropriate retarded time integrals. This leads to the requirement for knowledge of the fourth derivative of a fourth order correlation function in the turbulent flow. Not surprisingly, estimation of this function is difficult, but some success has certainly been achieved using this approach. The present report emphasizes the evaluation of the noise field via spectral methods. Thus the turbulence field is described by its wave-number and frequency characteristics rather than in space and time. One representation is simply the Fourier transform of the other, but it does appear that spectral methods offer considerable simplicity, and possibly also greater insight into the problem.

Most of the results previously found in jet noise theory can be rediscovered by a very simple spectral approach, and will be presented in the report. The simplicity is thought to be an important advantage. The present work has also enabled direct estimates of the noise to be made, as will be discussed in a later section. The work also suggests some experimental measurements of turbulence which appear to be particularly relevant to the noise problem.

2.0 BASIC MECHANISMS

2.1 The Lighthill Equation

The clearest way to understand the mechanisms underlying noise generation by turbulent flows is via the basic equation first derived by Lighthill (Reference 1). This equation has been the basis for virtually all work on exhaust noise to date. It can be derived in a straightforward way from the two basic conservation equations in fluid dynamics, for mass and momentum respectively. The equation for mass conservation (the continuity equation) can be written, in tensor notation with the summation convention, as

$$\frac{\partial \rho}{\partial t} + \frac{\partial \rho v_i}{\partial x_i} = Q \qquad (1)$$

where ρ is the density

t time

$v_i (i = 1,2,3)$ a cartesian velocity component

$x_i (i = 1,2,3)$ a three-dimensional cartesian coordinate

Q a rate of introduction of mass per unit volume which can vary with spatial position $\underset{\sim}{x}$.

The equation for conservation of momentum can be written, in Reynolds' form, as

$$\frac{\partial (\rho v_i)}{\partial t} + \frac{\partial \rho v_i v_j}{\partial x_j} + \frac{\partial p_{ij}}{\partial x_j} = F_i \qquad (2)$$

where $F_i (i = 1,2,3,)$ are the components of external force per unit volume acting over the fluid, and

$p_{ij} (i,j = 1,2,3,)$ is the nine-component stress tensor which includes both viscous stresses and internal pressure forces on the fluid.

Differentiating Equation (1) with respect to t and Equation (2) with respect to x_i and subtracting gives

$$\frac{\partial^2 \rho}{\partial t^2} = \frac{\partial Q}{\partial t} - \frac{\partial F_i}{\partial x_i} + \frac{\partial^2}{\partial x_i \partial x_j} (\rho v_i v_j + p_{ij}) \tag{3}$$

Now the "trace" of p_{ij}, that is the terms for which $i = j$, is essentially the scalar internal pressure which acts on the fluid. Here we are interested in calculating the sound, and therefore in the fluctuating part of Equation (3). As is well known the fluctuating pressure and velocity at a point in a homogeneous isotropic medium with speed of sound c are related by $p = c^2 \rho$. Thus, Lighthill (Reference 1) subtracted the term $c_0^2 \partial^2 \rho / \partial x_i^2$ from each side of Equation (3), with the result,

$$\frac{\partial^2 \rho}{\partial t^2} - c_0^2 \frac{\partial^2 \rho}{\partial x_1^2} = \frac{\partial Q}{\partial t} - \frac{\partial F_i}{\partial x_i} + \frac{\partial^2 T_{ij}}{\partial x_i \partial x_j} \tag{4}$$

where $T_{ij} = \rho v_i v_j + p_{ij} - c_0^2 \rho \delta_{ij}$

$\delta_{ij} = 1, \; i = j; = 0, \; i \neq j$ (The Kronecker δ)

Equation (4) will be termed the "Lighthill Equation". It can be seen that the left hand side of the Lighthill equation (4) is simply the wave equation, so that the right hand side gives the effect of various possible types of acoustic source. The Lighthill equation gives an expression therefore of the sound generation by various types of sources in an infinite homogeneous isotropic acoustic medium.

Each term on the right hand side of Equation (4) gives the effects of a different acoustic source mechanism. The first, $\partial Q / \partial t$ gives the effect of mass introduction. Examples include pulse-jets, sirens, tip jet rotors, and the random mass fluctuations that can occur across the exit plane of a jet exhaust. The second term, $\partial F_i / \partial x_i$ gives the effect of external fluctuating forces which can act on the air. Examples include compressors, propellers, helicopter rotors, and the random fluctuating forces that exist on the exhaust lip or on any body in a turbulent airstream. The third term $\partial^2 T_{ij} / \partial x_i \partial x_j$ incorporates several different effects. T_{ij} is generally referred to as the "Acoustic Stress Tensor," and can have nine components. In many cases the

most significant fluctuation of the acoustic stress tensor will be caused by turbulent velocity fluctuations which affect the $v_i v_j$ product. Virtually all calculations of noise radiation by turbulent velocity fluctuations have therefore utilized the Lighthill equation with T_{ij} put equal to $\rho_0 v_i v_j$. This approach has given considerable success in predicting basic trends of turbulence induced noise, and has also succeeded in predicting actual noise levels in some cases.

However, the remaining terms in the acoustic stress tensor T_{ij} justify closer study. The off-diagonal terms of $p_{ij}(i \neq j)$ represent viscosity induced stresses and will rarely be significant. Similarly any bulk viscosity effects on the diagonal terms ($i = j$) can be neglected. However, in a real inhomogeneous flow the possibility exists that $p \neq c_0^2 \rho$. Also the variable ρ appears in the $\rho v_i v_j$ term. Thus it is possible that ρ can have first order effects on the right hand side of the equation as well as on the left.

The Lighthill equation can be rewritten so that all possible effects of varying density are brought onto the left hand side of (4), which thus becomes an equation for inhomogeneous convected waves. This was done by Phillips (Reference 3). Unfortunately the resulting equation is almost impossible to solve even for the simplest types of acoustic source. For the types of source existing in a turbulent fluid it is doubtful if that equation can ever be solved exactly.

Thus in most work to date the effects of mean inhomogeneity on the flow have been tacitly ignored. The Lighthill equation is exact and does, in principle, contain these terms. However, the Lighthill equation is inevitably solved via the homogeneous retarded potential solution to the wave equation, with the right hand side being assumed known. Exact definition of the right hand side presumes knowledge of the necessary solution. Thus the first order approximations made in the solution will nearly always discard any possible acoustic effects of mean flow inhomogeneity.

The overall acoustic effects of inhomogeneities may be estimated by simple arguments. Consider a geometrical acoustics type of approximation to the inhomogeneous solution, where the speed of sound at any location is considered to be the sum of the local speed of sound and the local convection velocity. Thus the effective local speed of sound for an eddy moving at Mach 1 can actually be double the homogeneous value usually assumed. Sound may then be considered to travel along some ray path bent in accordance with the local effective speed of sound. For very low frequency sound, with wavelengths much greater than the jet dimension, the effect of ray bending will be negligible. Thus the first order solution to the Lighthill equation may be expected to apply either at low frequencies, or low exhaust velocities ($M << 1$). Again at high frequencies when the inhomogeneity has a scale much greater than the wavelength, the Lighthill equation will apply locally. Thus it should predict overall power correctly, provided a local wave equation is used.

On the other hand the directionality pattern of the noise in this case must be modified substantially due to the surrounding refraction zone. But at mid frequencies, where inhomogeneity scale and wavelength are of the same order, no definite rules can be laid down.

The redirectioning of sound due to refraction has been studied by several authors (References 4-18), and it appears that refraction may in reality be the principal cause of the observed directionality patterns of jets. No calculations of acoustic power appear to have been performed including this effect, but Powell and Ribner (References 20,21) have pointed out that the well known U^8 law, originated by Lighthill would continue to apply at the highest frequencies, since all basic parameters retained the same velocity dependence. At the lowest frequencies the U^8 law would again apply together with the $(1 - M_r)^{-5}$ dependency given by Ffowcs Williams (Reference 19) following Lighthill (Reference 2). But at the mid frequencies only a partial effect of the $(1 - M_r)^{-5}$ term could be expected, and at high frequencies zero effect.

In spite of the shortcomings of the Lighthill equation (4) discussed above, it will be the basis of the theoretical work presented in this report. This is because it does contain the first order effects which might be expected in practice and because no complete study of its first order implications is yet available. Note that the aerodynamic effect of inhomogeneities can be included in the aerodynamic source terms of T_{ij}, but that these sources are then considered to be operating in a uniform acoustic medium at rest, so that the "acoustic" effects of inhomogeneities are not incorporated.

2.2 Solution of the Lighthill Equation

If the right hand side of the Lighthill equation (4) is assumed known then its first order solution discussed in Section 2.0 is straightforward. First write the right hand side as $G(\underset{\sim}{y},t)$, so that G can represent any desired source term. The solution to the wave equation is well known from classical physics as

$$\rho(\underset{\sim}{x},t) = \frac{1}{4\pi c^2}\int \left[\frac{G(\underset{\sim}{y},t)}{r}\right] d\underset{\sim}{y} \qquad (5)$$

where the volume integral is over all $\underset{\sim}{y}$ space. The square brackets require that G must be evaluated at a retarded time $t' = t - r/c$. The symbol $\sim$ denotes a vector or tensor quantity, and is utilized because it requires the printer to reproduce the symbol in boldface (Clarendon) type, as is used for vectors. Note also the subscript of c_0 will be dropped for convenience for the rest of this report, except for discussions in Section 3.4.

It is of particular interest to study the spectral form of this solution. The Fourier transform pair relating G and its wave-number-frequency spectrum $\hat{G}$ are

$$\hat{G}(\underset{\sim}{k},\omega) = \iint G(\underset{\sim}{x},t) \exp - 2\pi i(\underset{\sim}{k}\bullet\underset{\sim}{x} + \omega t)\, d\underset{\sim}{x}\, dt \tag{6}$$

$$G(\underset{\sim}{x},t) = \iint \hat{G}(\underset{\sim}{k},\omega) \exp 2\pi i(\underset{\sim}{k}\bullet\underset{\sim}{x} + \omega t)\, d\underset{\sim}{k}\, d\omega \tag{7}$$

and using (7) in (5) gives

$$p(\underset{\sim}{x},t) = \frac{1}{4\pi c^2}\iiint \frac{\hat{G}(\underset{\sim}{k},\omega) \exp 2\pi i(\underset{\sim}{k}\bullet\underset{\sim}{y} + \omega(t - r/c))\, d\underset{\sim}{y}\, d\underset{\sim}{k}\, d\omega}{r} \tag{8}$$

Now $r^2 = (x_1 - y_1)^2 + (x_2 - y_2)^2 + (x_3 - y_3)^2$

Put $r_1^2 = x_1^2 + x_2^2 + x_3^2$

Then $$r^2 = r_1^2 \left\{ 1 - \frac{2\underset{\sim}{y}\cdot\underset{\sim}{r}}{r_1^2} + O\left(\frac{y}{r_1}\right)^2 \right\} \tag{9}$$

Thus, applying a geometric far field approximation, $y << r_1$, and expanding Equation (9) gives

$$r \approx r_1 - \frac{\underset{\sim}{y}\cdot\underset{\sim}{r}}{r_1} \tag{10}$$

Equation (10) may be substituted into Equation (8) to give a far field approximation to the noise as

$$\rho(\underset{\sim}{x},t) = \frac{1}{4\pi c^2 r_1}\iiint G(\underset{\sim}{k},\omega)\exp 2\pi i \left\{\left(\underset{\sim}{k} + \frac{r\omega}{c r_1}\right)\cdot \underset{\sim}{y} + \omega\left(t - \frac{r_1}{c}\right)\right\} d\underset{\sim}{y}\, d\underset{\sim}{k}\, d\omega \tag{11}$$

Now $$\int \exp 2\pi i(\underset{\sim}{y}\cdot\underset{\sim}{x})\, dy = \delta(\underset{\sim}{x}) \tag{12}$$

so that Equation (11) may be integrated with respect to $\underset{\sim}{y}$ and $\underset{\sim}{k}$ to give

$$\rho(x,t) = \frac{1}{4\pi c^2 r_1}\int \hat{G}\left(-\frac{\omega \underset{\sim}{r}}{c r_1}\ \omega\right)\exp 2\pi i\omega\left(t - \frac{r_1}{c}\right) d\omega \tag{13}$$

from which we can identify

$$\rho(\underset{\sim}{x},\omega) = \frac{\exp -2\pi i\omega r_1/c}{4\pi c^2 r_1}\ \hat{G}\left(\frac{-\omega \underset{\sim}{r}}{c r_1},\ \omega\right) \tag{14}$$

Equation (14) is a key result, which does not appear to be widely known, although it was first found by Kraichnan (Reference 24) in 1953. The result gives the fluctuating density spectrum directly in terms of the wave-number frequency spectrum of the source function. The initial exponential is simply a phase factor. Note particularly that there are no integrals in Equation (14), and that the pressure at a particular point is governed only by a single wave vector $\omega \underset{\sim}{r}/cr_1$. Equation (14) therefore appears to offer a particularly attractive formulation for the prediction of exhaust noise.

If, as suggested by Equation (4), we define

$$G(\underset{\sim}{x},t) = \frac{\partial Q}{\partial t} - \frac{\partial F_i}{\partial x_i} + \frac{\partial^2 T_{ij}}{\partial x_i \partial x_j} \tag{15}$$

then, assuming relations of the form of Equations (6) and (7) between the direct and spectral forms of the source functions, we find

$$\hat{G}(\underset{\sim}{k},\omega) = -2\pi i\omega \hat{Q}(\underset{\sim}{k},\omega) + 2\pi i k_i \hat{F}_i(\underset{\sim}{k},\omega) - 4\pi^2 k_i k_j \hat{T}_{ij}(\underset{\sim}{k},\omega) \tag{16}$$

from which, the sound field is given by

$$p(\underset{\sim}{x},\omega) = \frac{\exp -2\pi i\omega r_1/c}{4\pi c^2 r_1} \left\{ -2\pi i\omega \hat{Q} - \frac{2\pi i\omega r_i \hat{F}_i}{c r_1} - 4\pi^2 \frac{\omega^2}{c^2} \frac{r_i r_j}{r_1^2} \hat{T}_{ij} \right\} \tag{17}$$

where all spectra are evaluated at $(-\omega \underset{\sim}{r}/cr_1, \omega)$, or more shortly

$$p(\underset{\sim}{x},\omega) = \frac{-\exp -2\pi i\omega r_1/c}{2c^2 r_1} \left\{ i\omega \hat{Q} + i\frac{\omega}{c} \hat{F}_r + 2\pi \frac{\omega^2}{c^2} \hat{T}_{rr} \right\} \tag{18}$$

where subscript r denotes the component in the direction $\underset{\sim}{r}$, that is in the direction of the observer.

In the above analysis, all spectra are first order, simply the Fourier transforms of the original functions. For random functions this representation does not give a meaningful result and, as is well known, a second order or power spectrum must be defined. The necessary analysis is given in more detail in Appendix A. Essentially the first order spectrum must be multiplied by its complex conjugate and a limit taken. Applying this process to Equation (18) the exponential phase factor will vanish with the result (assuming zero correlation between the various sources)

$$\hat{\hat{p}}(\underset{\sim}{x},\omega) = \frac{1}{4c^4 r_1^2}\left\{+\omega^2\,\hat{\hat{Q}} + \frac{\omega^2}{c^2}\,\hat{\hat{F}}_r + 4\pi^2\,\frac{\omega^4}{c^4}\,\hat{\hat{T}}_{rr}\right\} \tag{19}$$

where the double hat notation has been introduced for second order spectra.

2.3 Sound Field of a Point Source in Uniform Motion

In order to obtain a better understanding of the present spectral description of the sound generation process it is helpful to consider this description as applied to a point source in motion. Figure 1 gives a wave number frequency diagram of the process. Consider a point source emitting a signal at a single frequency ω_0. The Fourier transform of a point singularity is a constant, so that the representation of a point source of a single frequency on the wave number-frequency plane is simply a straight line parallel to the k-axis, as shown in Figure 1 .

Lines of constant slope through the origin on this plane are lines of constant velocity $u = \omega/k$. The line $\omega/k = c$ is of particular interest since, by Equation (14) the value of the field $(\hat{G})$ along this line gives the magnitude of the sound radiated in the k direction. (On the present diagram only a single component for $\underset{\sim}{k}$ is shown which corresponds to the component in the direction of the observer.) Consider next the wave number-frequency field, relative to some coordinate systems which now moves relative to fixed axes with uniform velocity component V in the k direction. The relation between the two fields is given by

$$\hat{G}_{\text{fixed}}(k, \omega + kV) = \hat{G}_{\text{moving}}(k,\omega)$$

Thus the field of the point source given relative to the moving axes by $\omega = \omega_0$, becomes $\omega = \omega_0 + kV$ relative to moving axes, the dashed line in Figure 1 . Hence, while the fixed source produces sound at frequency ω_0 and wave number $k_0 = \omega_0/c$, the moving source parameters ω,k are found, by geometry, as $k = \omega/c = (\omega - \omega_0)/V$, which gives

$$\omega = \frac{\omega_0}{1 - M_r}\,, \quad k = \frac{k_0}{1 - M_r} \tag{20}$$

These give the well known Doppler shift effect.

The amplitude of the sound radiated may also be found by a simple argument. Figure 2 shows an enlarged version of Figure 1 in which the incremental values are specifically displayed. For the stationary case the sound in the frequency increment $\delta\omega$ is given by the part of the wave number spectrum lying in δk_1. But in the moving case the wave number region of interest is δk_2 wide. The ratio of the amplitudes is thus $\delta k_2/\delta k_1$, which is in the ratio of k/k_0 in Figure 2, which is in turn given by Equation (20) as $1/1 - M_r$.

However, in general there is no reason to suppose that the value of $\hat{G}$ at k will remain equal to the value at k_0, so that the $(1 - M_r)^{-1}$ factor cannot be applied alone, except in the monopole case. Equation (16) shows how point dipole (force) and quadrupole (acoustic stress) fields would vary as k and k^2 respectively, and this should be included in the estimation of the amplitude.

Thus Equation (18) for the sound can be rewritten, to include the effects of motion as

$$p(\underset{\sim}{x},\omega) = \frac{1}{2c^2 r_1 (1 - M_r)} \exp\left(\frac{-2\pi i \omega_0 r_1}{c(1 - M_r)}\right)\left\{\frac{i\omega_0}{1 - M_r} Q + \frac{i\omega_0}{c(1 - M_r)} F_r + \right.$$

$$\left. + 2\pi \left\{\frac{\omega_0}{c(1 - M_r)}\right\}^2 T_{rr} \right\} \qquad (21)$$

where ω_0 is the frequency in the moving axes. All spectra are evaluated at $\left\{-\omega_0 \underset{\sim}{r}/cr(1 - M_r),\ \omega_0/(1 - M_r)\right\}$. In the above equation all the arguments presented above referred to velocity and wave vector components in the direction of the observer. Note also that the mass source term Q in Equation (21) corresponds to a mass source and not to a "simple monopole source" $q = \partial Q/\partial t$ which would have an overall $(1 - M_r)^{-1}$ dependence, rather than the $(1 - M_r)^{-2}$ found here.

Thus, we have recovered the well known dependence of point monopole, dipole and quadrupole sources as $(1 - M_r)$ to the -1, -2, and -3 power respectively. This also implies a $(1 - M_r)$ to the -2, -4, and -6 power for the intensity ($\sim$density^2) of the sound. But note that this only applies when the spectrum analyzed in Figure 1 can be meaningfully represented as a first order spectrum, as in the case for a point source. For a random variation in space and time only the second order "power" spectrum (see Appendix A) can be meaningfully represented on Figure 1. In this case the same arguments apply, but to the mean square of the signal. Thus a factor of $(1 - M_r)$ is lost from the intensity expression and the convection velocity dependence of monopole, dipole and quadrupole random sources is as $(1 - M_r)$ to

the -1, -3, and -5 power respectively, as first pointed out by Ffowcs Williams (Reference 19).

A further point of interest is the effect of supersonic speeds. As indicated in Figure 3, both positive and negative sound velocities can be found on the wave number frequency diagram. For subsonic sources the negative sound velocities are meaningless since the sound proceeds in the opposite direction to that of the observer. But at supersonic speeds such directions of propagation can still give rise to observed sound fields and must, therefore, be included.

By geometry, as before, we find two observed frequencies for any given direction at supersonic convection speeds

$$\omega = \frac{\omega_0}{M_r + 1} \qquad \omega = -\frac{\omega_0}{M_r - 1}$$

Both these factors can be applied in the basic equations as was done for the subsonic case.

The $(1 - M_r)$ amplitude factors discussed above apply directly to the point source (δ function) case. but are basically estimates of the effect of motion. As can be seen from Figure 2 , if a source with finite bandwidth ($\delta\omega$) was under study the direct integration of the sound along the ray would give the same effect because of the large area of the source region which contributes. These estimates may be expected to be fairly accurate if the basic source strength does not vary too much with k. For instance the quadrupole sound trends shown in Equation (16) does include two additional k factors, and the $(1 - M_r)^{-3}$ estimate applies providing T_{rr} does not vary significantly between the fixed and moving axes values of k.

A more realistic turbulence spectrum will have values at all points of the wave number-frequency plane. Figure 4 shows a typical case where contours of equal values of the spectrum function have been plotted. Clearly, at zero wave number very little sound would be radiated in this case. At subsonic speeds the whole pattern slides sideways to the right and more sound would be radiated. At transonic speeds the sound is given by values lying through the maximum region of the spectrum, and at supersonic speeds the sound again goes down.

From this discussion it should be clear that the apparent transonic singularity of a point source at $M_r = 1$ reflects only a breakdown of the estimation procedure. At the transonic condition the sound ray c and velocity line V are parallel, and intercept at infinity thereby giving infinite frequency - an ultrasonic catastrophe. However, even for a true mathematical point source the sound radiation would be entirely dependent on the asymptotic values of the δ function as k tended to

infinity. But in a more realistic case the source strength at sufficiently high wave number will always be zero, and the integration along the c ray will emphasize other parts of the wave number spectrum. No particular difficulty at transonic speeds therefore occurs.

A final point of considerable significance in much of the discussion which follows may also be made by reference to Figure 4. Note that at both subsonic and at supersonic speeds intercepts of the sound line with the spectrum near the origin are of the greatest importance for sound radiation. These correspond to the low wave numbers in the spectrum. Only at transonic speeds do all the wave numbers in the turbulence contribute equally. Because of the factor of k^2 in Equation (16) no sound is actually radiated at $k = 0$, but it will still generally be true to say that it is the lower wave number components of the turbulence which dominate the sound field.

3.0 DEFINITION OF THE SOURCE FUNCTIONS

3.1 General

The results found in the last section suggest that the sound field of any prescribed turbulence field can be found directly from its wave number - frequency spectrum. Thus the problem now hinges on the spectral estimation of the turbulence. Such estimation typically requires evaluation of convolution integrals, as discussed in Appendix A. More specifically, Equation (17) showed how calculation of the sound radiated by a jet required knowledge simply of $\hat{T}_{ij}(\underset{\sim}{k},\omega)$ at the points $(-\omega\underset{\sim}{r}/cr,\omega)$ in wave number-frequency space. Definition of this term requires further manipulations.

The equation for the acoustic stress tensor is

$$T_{ij} = \rho v_i v_j + p_{ij} - c^2 \rho \delta_{ij} \tag{22}$$

Regarding this stress tensor in Lighthill's original formulation, it is assumed that the viscous stresses are neglected because its effect is small compared to the inertial term. Furthermore, the flow is assumed to be isentropic at low Mach numbers. Therefore the sum of the last two terms in Equation (22) vanishes for a homogeneous medium. In hot jet exhausts, especially in rocket exhausts, very complicated thermal fluctuations are presented. The isentropic flow assumption is not valid and the thermal effects emerge and become important, as discussed in Section 2.1.

The inertial term, $\rho_0 v_i(\underset{\sim}{x},t) v_j(\underset{\sim}{x},t)$, is a product of two quantities. Its spectrum is thus given by a convolution, Equation (A8) of Appendix A,

$$\hat{T}_{ij}(\underset{\sim}{k},\omega)_{\text{Inertial}} = \rho_0 \hat{v}_i(\underset{\sim}{k},\omega) * \hat{v}_j(\underset{\sim}{k},\omega) \tag{23}$$

or in the longer form, Equation (A5),

$$\hat{T}_{ij}(\underset{\sim}{k},\omega)_{\text{Inertial}} = \rho_0 \int_{\underset{\sim}{\ell}} \int_{\alpha} \hat{v}_i(\underset{\sim}{\ell},\alpha)\, \hat{v}_j(\underset{\sim}{\ell}-\underset{\sim}{k},\omega-\alpha)\, d\underset{\sim}{\ell}\, d\alpha \tag{24}$$

So that, if the first order spectra $\hat{v}_i$ are known, then the spectrum $\hat{T}_{ij}(k,\omega)_{\text{Inertial}}$ can be calculated.

It is common in jet noise theory to split the velocity v_i nto mean and fluctuating parts $v_i = U_i + u_i$, thus

$$\rho_0 v_i v_j = \rho_0 (u_i U_j + u_j U_i + u_i u_j) \tag{25}$$

where the mean value $U_i U_j$ has been discarded since it does not contribute directly to the sound.

Clearly the convolution integral Equation (24), will apply separately to each of the terms in Equation (25). On contraction $u_i U_j$ cannot be distinguished from $u_j U_i$ so that the first two terms may be construed as a single contribution which is due to the interaction of the turbulence and mean shear (T-M). The last term $u_i u_j$ gives the sound due only to turbulence-turbulence (T-T) interactions. Clearly the T-T contribution to $\hat{T}_{ij}$ is given by Equation (24) with $\underset{\sim}{v}$ replaced by $\underset{\sim}{u}$.

The two contributions will be defined as the "shear noise" and "self noise" respectively. These two terms together with the thermal effects on the sound source will be discussed separately in further detail.

3.2 Shear Noise

In order to evaluate the effect of the T-M term it is convenient to utilize a different version of the classic source term. From the derivation of Equation (16) it is clear that an alternative form of the spectral source term for turbulence is

$$\hat{G}(\underset{\sim}{k},\omega) = -2\pi i\, k_i \frac{\partial T_{ij}}{\partial x_j}\,(\underset{\sim}{k},\omega) \tag{26}$$

Now putting $T_{ij} = 2\rho_0 U_i u_j$

$$\hat{G}(\underset{\sim}{k},\omega) = -4\pi i \rho_0 k_i \left\{ U_i \frac{\widehat{\partial u_j}}{\partial x_j} + u_j \frac{\widehat{\partial U_i}}{\partial x_j} \right\} \tag{27}$$

The first term is zero by continuity. The second term is zero unless some mean shear is present, so that the description shear noise is appropriate for sound radiation due to

this effect. A convenient, and commonly used, assumption for further discussion is that the shear is a constant s_{ij}. The spectral source term then becomes

$$\hat{G}(\underset{\sim}{k},\omega) = -4\pi i \rho_0 k_i s_{ij} \hat{u}_j(\underset{\sim}{k},\omega) \tag{28}$$

A feature of this shear noise source is that only a single wave number term k_i multiplies the spectrum. Thus, following the arguments of Section 2.3, a $(1-M_r)^{-3}$ law will apply rather than the $(1-M_r)^{-5}$ law more usual for turbulence generated sound. This result was recently given, by a different argument, by Jones (Reference 30). The shear noise term is, in many ways, essentially dipole rather than quadrapole. But note the argument in Section 4.2 where a $(1-M_r)^{-5}$ law is found for the shear noise due to the presence of additional factors of k in the $\hat{u}_j$ spectrum.

In many jet flows intense turbulence will be limited to a region when the shear can reasonably be approximated as a constant, so that all the above results should apply. Note that if the shear dominates in a single direction then only that single component of the turbulence will interact with it to produce noise. A point of particular interest is that, under the constant shear assumption, only a direct spectrum of the turbulent is required. Shear noise is therefore simpler to estimate. If the shear cannot be taken as constant then a convolution between the turbulent and shear spectra becomes necessary, and the implications of this will be discussed at the end of the next section.

3.3 The Self Noise

As mentioned in 3.1, the source of the self noise term is given by Equation (24) with v replaced by u:

$$\hat{T}_{ij}(\underset{\sim}{k},\omega) = \rho_0 \int_{\underset{\sim}{\ell}} \int_{\alpha} \hat{u}_i(\underset{\sim}{\ell},\alpha)\, \hat{u}_j(\underset{\sim}{k}-\underset{\sim}{\ell},\omega-\alpha)\, d\underset{\sim}{\ell}\, d\alpha. \tag{29}$$

Upon multiplication with the directional unit vectors $k_i k_j$, the effective noise generating component in the turbulence strucrure is the self-convolution of the velocity spectrum in the direction of sound emission. Furthermore, only the points in the longitudinal direction of wave number k_r contributes to sound. The labor of integral calculation can thus be greatly reduced:

$$\hat{T}_{rr}(k_r, \underset{\sim}{k}_T = 0, \omega) = \rho_0 \int_{\underset{\sim}{\ell}} \int_{\alpha} \hat{u}_r(\ell_r, \underset{\sim}{\ell}_T, \alpha)\, \hat{u}_r(k_r - \ell_r, \underset{\sim}{\ell}_T, \omega - \alpha)\, d\ell_r\, d\underset{\sim}{\ell}_T\, d\alpha \qquad (30)$$

where the subscript T denotes the wavenumber vectors transverse to the sound emission direction. A substantial reduction of computation is realized because only one instead of nine integrals needs to be calculated. Within the multiple integral, the integration along the two ℓ_T directions represents a sum of squares instead of a convolution, and the evaluation of such an integral is usually much easier.

The source terms given both here, and in the preceeding section, are first order spectra, so that effects such as phase and skewness of the turbulence are reflected in the spectral parameters. For random variables it is, of course, necessary to take the average values of the square of this spectrum to give a second order power spectrum. However, this process will not alter the basic trends of any effects observed in the first order spectra.

It is worthwhile, at this point to contrast the results for self and shear noise. As was pointed out in Section 2.3, it is essentially the lower wave numbers of the turbulence which contribute to the sound heard in most parts of the acoustic field. Since the self noise is a self convolution the results at the low wave numbers are close to being the integral of the square of the first order spectrum, and even high wave numbers in the original turbulent field can give rise to low wave number intensity after self convolution. Also, it can be seen that the results will be comparatively insensitive to the detailed wave number pattern of the turbulence, and depend more on its mean level.

In the shear noise case the effect of a constant mean shear is to allow the turbulence to radiate directly. Lighthill (Reference 2) described the effect as an "aerodynamic sounding board." Here again we expect the lower wave numbers to radiate preferentially, but in this case radiation of the low wave number turbulence - for instance by breaking up the exhaust flow with splitters - should also reduce the noise. Also, the intensity of the noise is a function of the mean shear, so if that is reduced then noise should be also. A reduction in shear noise appears to be possible both by reducing the absolute magnitude of the shear, and by changing its distribution. If the shear region has the same dimensions as that of important contributions to the turbulence then the wave number convolution process will give large contributions near zero wave number. Here again, splitting up the turbulent flow suggests itself as a possible noise control measure. These arguments all suggest that the effectiveness of current jet engine exhaust silencers may have been more due to their effect on shear noise than on self noise.

3.4 Sound Generation by Compressible Flows with Heat Addition

Calculation of the sound generated by hot jet exhausts, and particularly by rocket

flows require examination of radiation from a region where many complicating thermodynamic effects are acting. Direct use of Lighthill's equation will not give exact results, for the reasons discussed in Section 2, although it is, of course, formally correct and could form the basis for an iterative solution. To reiterate, the basic conditions for Lighthill's equation stipulates that the fluid properties in the jet are the same as the surrounding medium. Furthermore, the flow is assumed to be isentropic. Therefore, the second term in the acoustic stress tensor $(p_{ij} - c_0^2 \rho\delta_{ij})$ contains only the contribution from viscosity and thus was neglected in the Lighthill approach. These conditions can be met in the far field, however, they are not satisfied in the near field. Thus, to use the Lighthill's equation to describe the sound field, it is necessary to examine the source terms by including some thermal effects. Thus, we will again use Lighthill's equation to obtain a first order estimate of the sound radiated. An alternative approach is given by Peter and Cottrell (Reference 48).

There are two principal effects which appear to be of importance in hot flows. The first is the direct effect of fluctuating density on the sound. The second is the possibility of non-isentropic processes which can cause the local pressure to differ from the local density times local speed of sound squared. In order to separate these two effects the quantity $c^2 \rho\delta_{ij}$ is added and subtracted to the right hand side of Equation (4), and relevant terms are grouped together:

$$T_{ij} = \rho \left\{ v_i v_j + (c^2 - c_0^2)\, \delta_{ij} \right\} + \left\{ p_{ij} - c^2 \rho \delta_{ij} \right\} \tag{31}$$

where c is the local speed of sound, which will vary over space with the local temperature. Let us study first the second term in Equation (31) ignoring as usual the viscous terms in p_{ij} so that $p_{ij} \approx p\delta_{ij}$.

First, some well-known results relating thermodynamic variables for thermally perfect gases are required, (e.g., Reference 25). The differential notation will be used for the fluctuating part of a thermodynamical variable, and these fluctuating quantities are limited to small deviations from a reference local isentropic state.

$$\left.\begin{aligned} ds &= \frac{dq}{T} = c_v \frac{dp}{p} - c_p \frac{d\rho}{\rho} \\ \gamma &= c_p / c_v \\ R &= (\gamma - 1)\, c_v \\ p &= \rho R T \end{aligned}\right\} \tag{32}$$

where s is entropy, q is heat addition per unit mass, c_v is the specific heat at constant volume, c_p is the specific heat at constant pressure, γ is the ratio of specific heat, and R is the gas constant.

The entropy equation in Equations (32) gives

$$ds = \frac{dq}{T} = \frac{c_v}{p} \left\{ dp - \frac{\gamma p}{\rho} d\rho \right\} \tag{33}$$

Now define the local isentropic speed of sound c by

$$c^2 = \gamma p/\rho = \gamma RT \tag{34}$$

Then Equations (33) may be written as

$$dp - c^2 d\rho = \frac{p\, ds}{c_v} \tag{35}$$

or, by using Equation (32) as

$$dp - c^2 d\rho = (\gamma - 1)\, p\, dq \tag{35a}$$

Since only fluctuations are significant in Equation (35), and (35a) give alternative expressions for its last term, and are clearly due to the effects of locally non-isentropic processes, in particular heat addition. Thus, the second term of the acoustic stress tensor, denoted by subscript 2, may be expressed as

$$(T_{ij})_2 = \frac{p\, ds}{c_v} = (\gamma - 1)\, p\, dq \tag{36}$$

When the flow conditions in the source deviate from the isentropic condition, it appears that Equation (36) will enable the additional sound due to the entropy fluctuation or heat addition, for example combustion, to be estimated.

Lighthill (Reference 27) gave

$$\left[(p - p_0) - c_0^2 (\rho - \rho_0) \right] \delta_{ij} \approx \frac{p_0}{c_v} (s - s_0)\, \delta_{ij} \tag{37}$$

This is an approximation to Equation (35) and applies where the local mean variables p, c can be approximated by their values outside the flow p_0, c_0. This was a good approximation in the case studied by Lighthill in Reference 27, where the interaction of turbulence with sound or weak shock waves was investigated. But for a hot exhaust

flow the approximations are less valid. The internal pressure of the exhaust may well be close to atmospheric, but the speed of sound may be very different. For a rocket the internal speed of sound is about three times that of the ambient environment, so that the above approximate expression is not appropriate. However, Lighthill's conclusion that "those kinetic temperature variations which result from the (nearly adiabatic) pressure fluctuations in the turbulence can be neglected" still holds locally, since this statement applies equally well to the expressions given by Equation (31) or Equation (38) below.

Nevertheless, local density changes can still produce some sound even under isentropic conditions. The first term of T_{ij} gives contributions to the sound field from density changes that could be locally isentropic. For the present case the dominant contribution to the $v_i v_j$ term arises from the mean velocity in the direction of the flow, for simplicity only this term will be retained. Using the definition of c from Equation (34) the first term of Equation (31) can be written

$$(T_{ij})_1 = \rho \left\{ U^2 + \gamma R (T - T_0) \delta_{ij} \right\} \tag{38}$$

For one-dimensional flows (Reference 25) the total enthalpy is given by:

$$h = c_p T_t = c_p T + \frac{U^2}{2} \tag{39}$$

where T_t is the local total temperature. Hence by using this equation and the Equation (32) we have

$$(T_{ij})_1 = \rho \left\{ (\gamma - 1) c_p (T_t - T_0) \delta_{ij} - \left(\frac{3 - \gamma}{2} \right) U^2 \right\}$$

When either the density or the enthalpy fluctuates, the above expression provides a first order fluctuation quantity for $(T_{ij})_1$ relative to the magnitude of the fluctuations. However, it is important not to include the same contribution to the sound field more than once. Fluctuations in velocity are included via the standard self and shear noise calculation. Fluctuations in entropy and enthalpy are included in Equation (36). Thus variations in static temperature from either isentropic or non-isentropic sources are included and do not require further consideration. Since the mean quantities do not contribute to the sound generation, we may write the density fluctuation effect as in the following expression:

$$(T_{ij})_1 = d\rho \left\{ (\gamma - 1) c_p (T_t - T_0) \delta_{ij} + \left(\frac{3 - \gamma}{2} \right) U^2 \right\} \tag{40}$$

Thus finally, density and temperature effects on sound generation are given by Equations (37) and (40), or as follows:

$$(T_{ij})_{\text{thermal}} = d\rho \left\{ (\gamma-1)\, c_p\, (T_t - T_0)\, \delta_{ij} + \left(\frac{3-\gamma}{2}\right) U^2 \right\} + ds \left\{ p/c_v \right\} \delta_{ij}$$

$$= (T_{ij})_1 + (T_{ij})_2 \qquad (41)$$

When the spectra of the fluctuation quantities are known, the thermal noise sources can be estimated by using Equation (41). It now is possible to estimate the sound radiation in the far field due to thermal effects by incorporating the result from Equation (41) into the right hand side of Equation (18) as an additional sound source. Of course, the multiplicative factors for the convection velocity effect should be established for moving thermal sound sources in accordance with the discussion in Section 2.3.

4.0 PREDICTION

4.1 Turbulence Spectra

In order to calculate the sound radiated by a jet exhaust it is necessary to possess information on its turbulent parameters. This information is difficult to find. Most theoretical work on turbulence has emphasized the isotropic turbulence case, and although this has given useful insights, a jet exhaust flow is sufficiently non-isotropic to introduce important difficulties. Experimental studies of turbulence also suffer from an important drawback since available measuring devices record only a volume integral of the approaching turbulent field. Furthermore, measurements of jet turbulence are usually made in a fixed frame of reference past which the slowly developing turbulent structure is swept at high speed.

Theoretical relations which describe some of these effects can be written down, based on the work of Batchelor (Reference 36). The notation used here corresponds to that of the rest of the report. If the turbulent velocity component in the i direction is u_i, then by an obvious extension of Equations (A-11) to (A-13) a cross spectrum and cross correlation function can be defined respectively by

$$\hat{\tilde{U}}_{ij}(\underset{\sim}{k},\omega) = \underset{V,T\to\infty}{\text{Limit}} \frac{1}{VT}\left\{\hat{u}_i(k,\omega)\,\hat{u}_j^*(k,\omega)\right\} \tag{42}$$

and

$$\overline{U}_{ij}(\xi,\tau) = \underset{V,T\to\infty}{\text{Limit}} \frac{1}{VT}\left\{u_i(\xi,\tau)^*\, u_j(-\xi,-\tau)\right\} \tag{43}$$

where u_i u_j are assumed to act within the space-time volume VT.

$\hat{\tilde{U}}_{ij}$ is a nine-component cross spectrum and can vary in an arbitrary manner with the wave vector $\underset{\sim}{k}$. If the turbulence is isotropic, then the spectrum will be a function of the magnitude of $\underset{\sim}{k}$ only, and not direction. Thus, a "scalar spectrum" $E(k,\omega)$ can be defined by

$$E(k,\omega) = \int_{|\underset{\sim}{k}|=\text{const}} \hat{\tilde{U}}_{ii}(\underset{\sim}{k},\omega)\, d\underset{\sim}{k} \tag{44}$$

where the integration is carried out over a spherical surface for each value of $k = |\underset{\sim}{k}|$.

Most possible measuring devices for use in a turbulent flow measure a single integral parameter as a function of time. An ideal one-dimensional device, to which a hot wire closely approximates, measures the "one-dimensional velocity spectrum" $\phi_1(k,\omega)$, defined by

$$\phi(k_1, \omega) = \iint \hat{U}_{11}(k_1, k_2, k_3, \omega)\, dk_2\, dk_3 \tag{45}$$

Note that $\phi_1(k_1, \omega)$ will usually be quite different from the component of the three-dimensional spectrum $\hat{U}_{11}(k_1, 0, 0, \omega)$.

If the turbulence is assumed to be isotropic, then relations between the various spectra can be derived. The full cross-spectrum is related to the scalar spectrum by

$$\hat{U}_{ij}(\underset{\sim}{k}, \omega) = \frac{E(k, \omega)}{4\pi k^4} (k^2 \delta_{ij} - k_i k_j)$$

and the one-dimensional velocity spectrum is related to the scalar spectrum by

$$\phi_1(k_1, \omega) = \frac{1}{2} \int_{k_1}^{\infty} \left(1 - \frac{k_1^2}{k^2}\right) \frac{E(k, \omega)}{k}\, dk \tag{46}$$

or

$$E(k, \omega) = k^3 \frac{d}{dk} \left[\frac{1}{k} \frac{d\phi_1(k, \omega)}{dk}\right] \tag{47}$$

The basic condition of isotropy imposes very strong restrictions on the application of these formulae. Both the spectra $\phi_1(k, \omega)$ and $E(k, \omega)$ are positive functions for all k. Thus, when $\phi_1(k, \omega)$ is derived from $E(k, \omega)$ in Equation (46), the factor $(1 - k_1^2/k^2)/k$ acts as a band pass filter. A plot of this factor for various values of k is shown in Figure 6. It will be seen that it is very heavily weighted for low values of k_1. Note that $E(k, \omega)$ at any given value of k always has a larger contribution, the lower the value of k_1. Note also that the peak contribution to a given k_1 comes from a value of $k = \sqrt{3}\, k_1$. In other words, a hot wire in isotropic turbulence actually responds most strongly to wave numbers at 55° to the normal.

Although an arbitrary scalar spectrum function will always give an allowable one-dimensional velocity spectrum, the reverse is not true. Since $E(k,\omega)$ must always be positive, several limitations are imposed on the possible shape of $\phi_1(k,\omega)$. It must be a monotone decreasing function of k with its maximum at $k = 0$. In fact, many measured spectra are not of this form. This is extremely unfortunate as it suggests that the convenient assumption of isotropy cannot be applied. Thus, in turn, all the

convenient formulae above cannot be applied, and it becomes very difficult to estimate the spectral form in a given direction as required by acoustic theory of Section 2.0.

Nevertheless, some general conclusions can be drawn. Wills (Reference 34) has measured wave number spectra of the u_1 (axial) component of turbulence. He has kindly lent copies of his original data plots to the authors to allow further analysis. A contour plot is used to display the measured wave number spectrum in Figure 4. The vertical axis is wave number and is, of course, the wave number of the measured one-dimensional velocity spectrum. The horizontal axis, in convection velocity, obtained simply by dividing frequency by wave number. The overall convection velocity of the turbulence can be defined via the locus of maxima of the contours in the plot, and is shown in Figure 4.

The typical value of the convection velocity is 205 ft/sec which corresponds closely to the mean velocity at the measurement position. But clearly the convection velocity is also a function of wave number. A common assumption in turbulence theory is that the exhaust flow consists simply of a homogeneous decaying turbulence which is being convected. If the spectrum of Figure 4 is replotted relative to its moving frame of reference as a function of wave number, then the result shown in Figure 5 is obtained. The intensity contours are symmetric with respect to frequency as measured relative to the moving frame. This result does justify the convecting assumption, which has already been used extensively in Section 2.3.

Another point of interest is the very rapid decay of the turbulent energy with higher convection speeds. If the spectrum were of a true wave number component, then the energy at the speed of sound in the figure would be, identically, the sound radiated by the turbulence. Since the spectrum is actually an integral measurement, this identity is no longer true, but there is obviously a fairly direct connection between the energy at the speed of sound in this spectrum and the real sound generated.

Finally, it is necessary to specify some form for the turbulence spectrum in order to make an initial evaluation of the possible noise radiation field. At the present time, no available experimental data specifies the full three-dimensional turbulence to such a detail as required by the noise prediction theory. Nevertheless, the spectral noise prediction technique is applicable to any given turbulent jet model. It is intended here to choose a simple turbulence model which may bring out all the important aspects relative to sound radiation. It will be particularly beneficial to choose a model such that all subsequent analysis can be carried through in analytical form. We will be able to draw rigorous conclusions about the detail of noise generation mechanisms in the turbulence and features of the radiated sound field. One form of the central limit theorem (Reference 49) states that multiple convolution gives rise to Gaussian correlation functions. Since the final noise radiation is the result of at least four convolutions, it appears reasonable to take a simple error function curve for the form of the correlation, and thus also spectral, functions.

A simple isotropic turbulence structure, defined in the convected frame of reference, will be chosen. The spectral representation of this model is given by

$$\hat{U}_{ij}(\underset{\sim}{k},\omega) = \frac{a^3 \beta\, \bar{u}_0^2}{16\pi^2} \left\{(k a)^2 \delta_{ij} - a^2 k_i k_j\right\} \exp - \left\{(k a)^2 + (\beta\omega)^2\right\} \tag{48}$$

where $\bar{u}_0^2$ is the mean turbulence intensity, a is the integral spatial scale, and β is the integral time scale. All these three parameters can be adjusted to values of corresponding parameters in a typical jet. Experimental results (References 21-23) suggest that

$$\bar{u}_0^2 \simeq 0.09\, U^2 \tag{49}$$

and

$$\alpha = \frac{a}{c M \beta} \cong 0.20 \sim 0.35 \tag{50}$$

This spectral form, Equation (48), corresponds to the correlation description

$$\overline{u_i u_j}(\underset{\sim}{\xi},\tau) = u_0^2 \left\{\left(1 - \frac{\pi \xi^2}{\alpha^2}\right) \delta_{ij} + \frac{\pi^2}{a^2} \xi_i \xi_j\right\} \exp - \left\{\left(\frac{\pi\xi}{a}\right)^2 + \left(\frac{\pi\tau}{\beta}\right)^2\right\}$$

This model can easily be extended to a scale anisotropic turbulence, namely, a model using more than one spatial integral scale.

It is important to bear in mind that the chosen model of turbulence only resembles the turbulence structure in a real jet in its intensity and integral scales, and other features of possible importance are not incorporated.

4.2 Shear Noise

The analysis in Section 3.2 found that the shear noise is generated through the interaction between the mean flow shear gradient and the $u_2(k,\omega)$ component of the turbulence spectrum. In particular, the shear noise spectrum is directly proportional to $u_2(\underset{\sim}{k},\omega)$ when shear gradient is assumed to be constant. Hence, with the choice of turbulence model (48), the second order spectrum of the velocity fluctuation in the ξ_2-direction, $\hat{U}_2(\underset{\sim}{k},\omega)$, is

$$\overset{M}{U}_2(k,\omega) = \frac{c^3 \beta J_0^2}{16\pi^2} \left\{(k_1 a)^2 + (k_3 a)^2\right\} \exp - \left\{(ka)^2 + (\beta\omega)^2\right\} \tag{51}$$

The noise intensity is given by the following formula (Reference 23):

$$\overset{M}{I}(\underset{\sim}{x}_0, \omega) = c^3 \rho^{-1} \overset{M}{P}(k,\omega) \tag{52}$$

where $\underset{\sim}{x}_0$ denotes the location of an observer in the far field.

The cylindrically symmetric structure of a jet also requires consideration. The radiation direction of sound to a fixed observer from different small volumes of turbulence around a circular slice of jet will make different angles with the local normal of the shear flow. Hence, we shall first find the average contribution of shear noise sources of all orientations. If we denote

$$k_1 = k\cos\theta, \quad k_2 = k\sin\theta\cos\phi, \quad k_3 = k\sin\theta\sin\phi, \tag{53}$$

then the average shall be taken in the variable ϕ. The most convenient entry point for taking this average is Equation (51):

$$\frac{1}{2\pi}\int_0^{2\pi} \overset{M}{U}(k,\omega)\, d\phi = \frac{a^3 \beta \bar{U}_0^2}{16\pi^2} (ka)^2 \int_0^{2\pi} (\cos^2\theta + \sin^2\theta \sin^2\phi) \exp - \left\{(ka)^2 + (\beta\omega)^2\right\} d\phi$$

$$= \frac{a^3 \beta \bar{U}_0^2}{16\pi^2} (ka)^2 \left(\frac{1+\cos^2\theta}{2}\right) \exp - \left\{(ka)^2 + (\beta\omega)^2\right\} \tag{54}$$

Substituting (54) into Equation (19) and combining the result into Equation (52), we obtain the noise radiation intensity per unit volume of turbulence as

$$\overset{M}{I}(\underset{\sim}{x}_0, \omega) = \frac{\bar{U}_0^2 \rho \omega^2 a^3 \beta (ka)^2 (\cos^4\theta + \cos^2\theta)}{32\pi^2 c^3 r^2 (1 - M\cos\theta)^3} \left(\frac{\partial U_1}{\partial x_2}\right)^2 \exp - \left\{k^2 a^2 + \beta^2 \omega^2\right\} \tag{55}$$

The shear noise directivity pattern contained in Equation (55) agrees with the result given by Ribner in Reference 21.

Since,

$$k = \frac{-\omega}{c(1 - M\cos\theta)}$$

Equation (55) can further be simplified to

$$\overset{M}{I}(\underset{\sim}{x}_0, \omega) = \frac{\bar{v}_0^{\,2} a^5 \beta \rho \omega^4 (\cos^4\theta + \cos^2\theta)}{32 \pi^2 c^5 r^2 (1 - M\cos\theta)^5} \left(\frac{\partial U_1}{\partial x_2}\right)^2 \exp - \frac{\omega^2 a^2}{c^2} \left\{\frac{1}{(1 - M\cos\theta)^2} + \frac{1}{\alpha^2 M^2}\right\} \tag{56}$$

The noise intensity for any frequency band can readily be computed using Equation (56) and a simple integration. For example, the noise intensity for an octave band with center frequency ω_n is given by

$$I(\underset{\sim}{x}_0, \omega_n) = \frac{a^5 \beta \rho \bar{v}_0^{\,2} (\cos^4\theta + \cos^2\theta)}{32 \pi^2 c^5 r^2 (1 - M\cos\theta)^5} \left(\frac{\partial U_1}{\partial x_2}\right)^2 \int_{0.707\,\omega_n}^{1.414\,\omega_n} \omega^4 \exp - \frac{\omega^2 a^2}{c^2} \left\{\frac{1}{(1 - M\cos\theta)^2} + \frac{1}{\alpha^2 M^2}\right\} d\omega \tag{57}$$

where the subscript n for ω indicates the denumeration of the sequence octave bands.

In particular, when the wide band noise intensity is considered, the limits of the integration over ω goes from zero to infinity. In this case the resulting expression reads:

$$I(\underset{\sim}{x}_0) = \left(\frac{\partial U_1}{\partial x_2}\right)^2 \frac{3\sqrt{\pi}\,\rho\,\bar{v}_0^{\,2}\,\alpha^4 M^4 a (\cos^4\theta + \cos^2\theta)}{256 \pi^2 c\, r^2 \left\{(1 - M\cos\theta)^2 + \alpha^2 M^2\right\}^{5/2}} \tag{58}$$

It is interesting to investigate the noise source distribution in the wave number-frequency space. The spatial and the time factors of the noise source are plotted in separate figures. Figure 7 shows the turbulence intensity distribution in the k_1, k_2-plane. The wave number k_3 is set to zero for simplicity of representation. A vector OC is drawn along the direction of emission of the noise. In this figure, the source intensity is given along OC and several other representative sections. It is clear that the shear noise is zero in the transverse direction, k_2, and reaches a maximum in the axial direction, k_1.

An important feature not represented in Figure 7 is the location of noise source in the wave number space where the most intense sound radiation occurs. The definition of the turbulence structure, Equation (51), consists of separable wave-number and frequency factors. The peak turbulence intensity in the wave-number space is determined entirely by the wave number component. However, the most intense part of the turbulence spectrum does not necessarily generate the most intense sound. In

the formulation of shear noise, Equation (55), one may detect also two separable factors. In particular, the frequency factor is

$$f(\omega) = \omega^2 \exp - (\beta^2 \omega^2) \tag{59}$$

The variation of turbulence intensity with wave number along section OC, and the factor $f(\omega)$, are plotted in Figure 8 to the common abscissa $k = \omega/c(1 - M\cos\theta)$. Their product, plotted on the same figure, is proportional to the shear noise intensity.

The peak of $f(\omega)$ is located at $\omega = \beta^{-1}$. Since the intensity of the turbulence varies with k^2 in the low wave number range, its product with $f(\omega)$ produces a peak of shear noise at a frequency $\omega = \sqrt{2}\,\beta^{-1}$. The conclusion reached by this analysis shows that the location of sound of peak noise relative to the wave number space is dominated by the frequency factor in the case of shear noise.

For the shear noise, the effect that the noise peaks half an octave above the frequency factor is somewhat artificial. If the wave number spectrum were flatter in the low wave number range, instead of rising as k^2, the noise peak would be more or less coincident with the peak of the frequency factor. However, some general effect along the lines discussed is expected.

In Reference 21, Ribner established that the shear noise will peak at a frequency one octave below the peak frequency of the self noise. The argument was based on the frequency factor alone. This phenomenon is born out by experimental evidences. The present analysis leads to the same conclusion. However, it reveals that the physical mechanism is actually quite complex.

Finally, the dependence of the shear noise intensity on ω^4, Equation (56), instead of ω^2, is also due to the choice of the turbulence model. Had the turbulence intensity spectrum curve been flat in the low wave number range, the dependence would have been ω^2. This also affects the dependence on the convection factor $(1 - M\cos\theta)$. In Section 3 it was pointed out that the shear noise obeyed a $(1 - M_r)^{-3}$ law. In Equation (56) the shear noise is obeying a $(1 - M_r)^{-5}$ law. This is simply due to the two additional factors of k assumed in the present model of the turbulence.

4.3 Self Noise

In Section 3.4, it was found that the instantaneous self noise source spectrum is a self convolution of the spectrum of the fluctuating velocity component in the noise emission direction. It can be directly computed if the velocity fluctuation spectrum is known. In any case, the instantaneous sound source itself is a second order quantity. While the turbulent flucuations are random, one can only define, or make meaningful measurements of their mean square magnitude. In the case of self noise, we should deal with

$$\hat{\hat{T}}_{rr}(\underset{\sim}{k}, \omega) = \hat{T}_{rr}(\underset{\sim}{k}, \omega) \cdot \hat{T}_{rr}^{*}(\underset{\sim}{k}, \omega) \tag{60}$$

which is a fourth order quantity. The corresponding correlation representation of this quantity is, by definition

$$\overline{T}_{rr}(\underset{\sim}{\xi}, \tau) = \overline{u_r^2(\underset{\sim}{y}_0, t)\, u_r^2(\underset{\sim}{y}_0 + \underset{\sim}{\xi}, t + \tau)} \tag{61}$$

From an experimental point of view, the fourth order spectrum $\hat{\hat{T}}_{rr}(k,\omega)$ can be measured directly (Reference 40). For the present example, it is desirable to compute this quantity from the chosen model of turbulence. Here, it is necessary to assume that in the turbulence the velocity fluctuations at any two points are jointly normal in probability. However, such an assumption must be used with care, as discussed by Proudman (Reference 50).

By employing the above assumption, Batchelor (Reference 36) shows that Equation (61) can be reduced to

$$\overline{T}_{rr}(\underset{\sim}{\xi}, \tau) = \overline{u_r^2}^2 + 2\left\{\overline{u_r}(\underset{\sim}{\xi}, \tau)\right\}^2 \tag{62}$$

where $\overline{u_r^2}^2$ is a constant and irrelevant to sound generation.

Now the fourth order spectrum of $\hat{\hat{T}}_{rr}(\underset{\sim}{k}, \omega)$ can be evaluated by means of a convolution of the known turbulence spectrum $\hat{\hat{u}}_r(\underset{\sim}{k}, \omega)$:

$$\hat{\hat{T}}_{rr}(\underset{\sim}{k}, \omega) = \iint_{\underset{\sim}{\ell}\ \sigma} \hat{\hat{u}}_r(\underset{\sim}{\ell}, \sigma)\, \hat{\hat{u}}_r(\underset{\sim}{k} - \underset{\sim}{\ell}, \omega - \sigma)\, d\underset{\sim}{\ell}\, d\sigma \tag{63}$$

In an isotropic turbulence structure the second order spectrum of a velocity component in any direction has the same form. Hence, the second order spectrum of velocity fluctuations in the direction of sound emission can be given as

$$\hat{\hat{u}}_r(\underset{\sim}{k}, \omega) = \frac{a^3 \beta \bar{u}_0^2}{16\pi^2}\left\{(ka)^2 - (k_r a)^2\right\} \exp - \left\{(ka)^2 + (\beta\omega)^2\right\} \tag{64}$$

The convolution integral as defined by Equation (63) is algebraically lengthy, though not difficult. If the cartesian coordinates are oriented such that the first axis points in the direction of sound emission $\underset{\sim}{r}$, the component of wave number in this direction will be k_r, and the wave number vector in directions perpendicular to the first axis

will be designated as $\underset{\sim}{k}_T$. The general formula for noise radiation states that the effective component of $\hat{\hat{T}}_{rr}(\underset{\sim}{k},\omega)$ as a noise source is restricted to $k_r = -\omega/c(1 - M\cos\theta)$, and $\underset{\sim}{k}_T = 0$. The integration of Equation (63) can be greatly simplified because the component $\underset{\sim}{k}_T$ of the parametric wave number $\underset{\sim}{k}$ can now be set to zero:

$$\hat{\hat{T}}_{rr}(k_r, k_T = 0, \omega) = \int_{\underset{\sim}{\ell}} \int_{\sigma} \hat{\hat{U}}_r(\ell_r, \ell_T, \sigma)\, \hat{\hat{U}}_r(k_r - \ell_r, -\ell_T, \omega - \sigma)\, d\ell_r\, d\ell_T\, d\sigma$$

The integration in these directions degenerates from a convolution to an operation of mean square sum. This can easily be seen if one omits the variables k_r, ℓ_r, ω, and σ from the above formula, and recalls that $\hat{\hat{U}}_r(\underset{\sim}{k},\omega)$ is an even function in all the variables.

Substituting Equation (64) into Equation (63), the spectrum $\hat{\hat{T}}_{rr}(k,\omega)$ can be written as

$$\hat{\hat{T}}_{rr}(k_r,\omega) = \frac{2\,\bar{u}_0^4\,(a^3\beta)^2}{(16\,\pi^2)^2} \int_{-\infty}^{\infty} (\ell_T a)^4 \exp - \left\{2(\ell_T a)^2\right\} \cdot \exp - \left\{(\ell_r a)^2 + (\sigma\beta)^2\right\}$$

$$\cdot \exp - \left\{(k_r - \ell_r)^2\, a^2 + (\omega - \sigma)^2\, \beta^2\right\} d\underset{\sim}{\ell}_T\, d\ell_r\, d\sigma \qquad (65)$$

where $\underset{\sim}{\ell}_T$ denotes the vector wave numbers which are transverse to the direction of sound emission, and ℓ_T denotes the magnitude of the vector $\underset{\sim}{\ell}_T$.

Upon evaluating the above convolution integral, the spectrum $\hat{\hat{T}}_{rr}(\underset{\sim}{k},\omega)$ as restricted to the k_r component is

$$\hat{\hat{T}}_{rr}(k_r,\omega) = \frac{a^3\,\beta\,\bar{u}_0^4}{512\,\pi^2} \exp - \frac{1}{2}\left\{k_r^2\, a^2 + \omega^2\,\beta^2\right\} \qquad (66)$$

Using Equations (19), (52), and (66), and go through similar steps of computation as in the shear noise case, the noise intensity per unit volume of source is

$$\hat{I}(x_0, \omega) = \frac{1}{(1 - M\cos\theta)^5} \frac{\bar{v}_0^4 \rho \omega^4 a^3 \beta}{128 c^5 r^2} \exp - \frac{1}{2} \frac{\omega^2 a^2}{c^2} \left\{ \frac{1}{(1 - M\cos\theta)^2} + \frac{1}{\alpha^2 M^2} \right\} \quad (67)$$

Similarly, the broad band intensity can be obtained by integrating (67) over frequency ω.

For an octave band with center frequency ω_n, the expression is

$$I(\underset{\sim}{x}_0, \omega_n) = \frac{\rho \bar{v}_0^4 a^3 \beta}{128 c^5 r^2 (1 - M\cos\theta)^5} \int_{0.707\,\omega_n}^{1.414\,\omega_n} \omega^4 \exp - \frac{1}{2} \frac{\omega^2 a^2}{c^2} \left\{ \frac{1}{(1 - M\cos\theta)^2} + \frac{1}{\alpha^2 M^2} \right\} d\omega \quad (68)$$

For the overall noise intensity, the result after integration reads

$$I(\underset{\sim}{x}_0) = \frac{3\sqrt{2\pi}\, \rho v_0^4 \alpha^4 M^4}{256\, a c r^2 \left\{ (1 - M\cos\theta)^2 + \alpha^2 M^2 \right\}^{5/2}} \quad (69)$$

The directional variation of the noise intensity for fixed r comes entirely from the convection effect, because the source is isotropic in the moving frame of coordinates.

When the noise source term is broken down into its spatial and time factor, we see again that the time factor decides the location of the peak noise frequency. The distribution of $\hat{u}_r(\underset{\sim}{k}, \omega)$ and $\hat{T}_{rr}(\underset{\sim}{k}, \omega)$ in the k_r, k_T, plane are shown in Figure 9. The general topography of the fourth order spectrum is markedly different from the second order spectrum. The time factor

$$f(\omega) = \omega^4 \exp - \frac{1}{2} \beta^2 \omega^2 \quad (70)$$

is plotted in Figure 10 together with $\hat{T}_{rr}(k_r, 0)$ and the noise spectrum given by the product of the frequency factor and the spatial factor. The frequency factor $f(\omega)$ has a peak located at $\omega = 2/\beta$ which is exactly one octave above the corresponding peak of frequency factor for the shear noise. Since the self noise spectrum at low wave numbers is quite flat due to the self convolution, the location of peak noise more or less corresponds to the peak of $f(\omega)$. Hence, the peak self-noise frequency is between $\sqrt{2}$ and 2 times as high as the shear noise, depending on the flatness of the basic wave number spectrum as discussed in Section 4.2.

We find, from the convolution integral, Equation (65), that the sound source depends on the self-convolution of the second order spectrum in the longitudinal direction and the sum of square of the same spectrum in the transverse directions. The strength of the noise source is therefore relatively insensitive to the assumed form of the turbulence structure as long as the total power remains the same. In view of this property, one may expect that a simple model of turbulence may provide a good prediction of the self noise.

4.4 Comparison with Existing Experimental Results and Possible Further Experiments

Equations (57), and (58) of Section 4.2 and Equations (68) and (69) of Section 4.3 represent some final results of noise radiation prediction out of an assumed model jet. These equations can be applied immediately to numerical computations. For a given set of jet parameters, predictions can be made on the directivity pattern of overall far field sound pressure level, octave band sound pressure levels, and the overall acoustic power output. The required input data contains simply the jet diameter, exit velocity, integral spatial and time scales of the turbulence model, the parameter α, and physical constants of the surrounding medium.

Some jet noise experimental data are available for comparison with theoretical predictions. Both sets employed below are obtained under controlled laboratory conditions. For in practical cases, jet noises are often accompanied by other intensive sources of noise. Notably, in the case of a real jet engine the compressor noise is just as powerful as the jet noise, and can cause difficulties in interpretation.

As a first example, the sound field parameters are computed for a jet of one inch diameter, with exit Mach number of 0.80. The results of computation are shown in Figure 11. For the same jet diameter and exit speed, Mollo-Christensen (Reference 39) has measured the overall noise intensity, and separately noise intensities in the low frequency range and the high frequency range of the noise spectrum. He finds that in the low frequency range the noise is predominantly directed forward, while in the high frequency range a peak appears at about 45 degrees from the jet axis. According to theoretical analysis, the low frequency noise is mainly produced by the shear gradient and turbulence interaction mechanism. Since the frequency is very low, it is less affected by the refraction effects of the mean flow. Hence, this set of measurements can be compared to our shear noise computation. On the other hand, the high frequency portion of the noise spectrum is greatly refracted. The appearance of a peak at 45 degrees is generally considered as a result of refraction (see discussion in Section 2.1).

The rms sound pressure given in Reference 39, however, is in terms of milli-volts of the signals from the microphone. Hence, the comparison between theory and experiment can only show trends at best. The data of measurement and the computation from the present theory are matched at a point on a 45 degree radial line. The sound intensities inferred from the data for the overall noise and the noise in the low frequency range compare favorably with our computation of overall noise and shear noise, respectively.

The second set of data considered here is the jet noise measurements obtained by Mangiarotty et al. (Reference 38). This report presents a more systematic collection of results about far field jet noise radiation. The experimental program is intended for evaluation of various designs of noise abatement exit nozzles. Three special nozzle designs are tested against a smooth conical nozzle, which has an area of 6.42 square inches and a diameter of 2.86 inches. With the smooth nozzle, the overpressure in the reservoir has been adjusted to three level to provide jet exit Mach numbers of 0.50, 0.80, and 0.90. Sound pressure levels are recorded simultaneously by a series of microphones along a straight line ranging from 2 to 18 feet from the nozzle exit.

For each of the three run conditions, sound pressure level directivity patterns are measured for noise in nine consecutive octave bands (Table I), and for the overall noise. The results are presented in a series of graphs. The general trend shows again that the low frequency noise has a predominantly forward pattern, and the high frequency noise pattern has a peak near the 40-degree direction. The refraction effects begin to appear near the characteristic frequency of the jet.

Far field noise radiation prediction has been made for one case where $M = 0.80$ (Pressure head = 13.5 inches Hg). Computations for sound pressure level cover similar octave bands as in the experiment. The numerical results, together with experimental data from Reference 38, are shown in Figures 12 and 13.

Figure 12 shows that overall levels are predicted to within 5 dB over the whole acoustic field. This is thought to be a significant result. It will be observed that the spectral shape prediction of the theory are considerably less accurate. However, the present work used a much simplified spectral model for analytic convenience, and many improvements are clearly possible. The prediction and experimental data agree well in the octave bands where the peak noise intensities occur. But for high frequency bands the predictions are very poor. In the chosen model of turbulence, the frequency spectrum drops off much faster than any actual turbulence structure.

One can recognize in Equations (57), (58), (68), and (69) that the turbulence scales a, β, and the constant parameter α are very important in noise prediction. These parameters can only be confirmed by experiments. Moreover, we should hardly be satisfied with the simple estimation made possible by assuming an isotropic turbulence model.

Although extensive data on jet turbulence are available in the literature, most are not applicable to predictions of jet noise. The reason is either that the measured turbulence component is not directly related to sound generating elements, or that the measurement is not sufficiently accurate in the low wave number range to render meaningful sound radiation estimates. The only exception so far is the experimental work by Chu (Reference 40). This study was specifically designed according to basic jet noise theory.

Chu measured the space-time correlation functions $\overline{T_{rr}}(\underset{\sim}{\xi},\tau)$ and $\overline{u_r}(\underset{\sim}{\xi},\tau)$ in several orientations of $\underset{\sim}{r}$ with a pair of single-wire hot wire anemometers. Corrections are made for the effect of mean convection velocity in the mixing region. Chu based his work on jet noise theory in its correlation form, which predicts noise by means of an integration of the fourth time derivative of the space time correlation functions. This approach is equivalent to assuming that the noise is generated by the zero wave number component of the turbulence. Hence the above obtained data is not further analyzed in spectral form. Instead, a numerical smoothing scheme is judicially chosen to handle the derivatives and integration. The important information of the spectral content, which could be obtained from measurements of this type, are not preserved.

In this set of measurements, the $\overline{u_2}(\underset{\sim}{\xi},t)$ component of the turbulence was not measured. This is partly due to the instrumentation employed by Chu, because a cross wire probe is necessary for such measurements. It is clear in the present theory that this component of turbulence is essential in the prediction of shear noise.

It should be noted here that Chu's work has made significant contribution towards resolving the very difficult problem of measuring fully three-dimensional jet turbulence structure. The above discussions serve only as guide-lines to further investigations.

In addition to the above mentioned general shortcomings of existing data on jet turbulence, one important aspect has been ignored altogether. It is familiar that the turbulence intensity across the jet is non-uniform. This spatial inhomogeneity of the turbulence structure has a profound influence on the spectrum of the turbulence according to theories of spectral analysis. This effect is particularly important for the low wave number range, where most sound is generated. The inhomogeneity must therefore be considered thoroughly in both the experimental design and the data analysis phases of the experimental program.

The following quantities require definition:

a. The fourth order spectrum $\hat{\hat{T}}_{rr}(\underset{\sim}{k},\omega)$ for various values of r orientation;

b. The mean flow velocity profile $U_1(\xi_2)$;

c. The transverse velocity fluctuation spectrum $\hat{\hat{u}}_2(\underset{\sim}{k},\omega)$;

d. The turbulence intensity profile of the jet $\bar{u}_0^2(\xi_2)$.

Some data on all these parameters exists except for the transverse spectrum. This is important for the shear noise estimation and justifies careful experimental study. When the data from the above set of measurements is properly analyzed and organized, the jet noise can be estimated through the application of the present theory.

5.0 SUMMARY AND CONCLUSIONS

Space/time spectral analysis techniques have been used in an attempt to understand and predict the noise from turbulent exhaust flows. A unified theory has been derived, based on Lighthill's Equation, in which shear noise, self noise, and non-isentropic noise generation can be described. It appears that the present spectral techniques can give a simple, convenient and accurate theoretical description of the noise generating process from jet exhaust flows.

Several of the familiar results in jet noise theory have been regenerated in a simple manner, and new insight has been gained into the basic mechanisms of the noise generating processes. The shear noise is found to be dependent on the detailed structure of the flow, while the self noise is found to be essentially independent. Thus, it appears that shear noise can be reduced by geometrical modifications to the exhaust flow, while the self noise can only be controlled by reduction of the turbulent intensities. The theoretical analysis also suggests that the peaks of the shear noise spectrum is somewhat less than one octave below that of the self noise.

Existing data on jet turbulence is inconvenient for estimation of noise radiation. However, data has been reviewed and its implications for jet noise discussed. Recommendations for experiments to gather more meaningful turbulence data for jet noise prediction are put forward.

Theoretical calculations of jet noise intensities have been made corresponding to two reported experiments. A simple analytical model of the turbulence was taken, but overall levels were found to agree within 5 dB over the whole noise field. Furthermore, the predictions agree well with experimental data in the octave bands where the peak noise intensities occur. The frequency spectrum shape was not predicted well, but this is thought to be due to the simplifying assumptions made in the present analysis. The agreement in overall level was achieved without the use of disposable parameters and justifies hope that more detailed theoretical calculations will enable the whole acoustic field to be predicted accurately from theory for the first time.

REFERENCES

1. Lighthill, M.J., "On Sound Generated Aerodynamically. I. General Theory," Proceedings of Royal Society, Series A, Vol. 211, 564-578 (1952).

2. Lighthill, M.J., "On Sound Generated Aerodynamically. II. Turbulence as a Source of Sound," Proceedings of Royal Society, Series A, Vol. 222, 1-32 (1954).

3. Phillips, O.M., "On the Generation of Sound by Supersonic Turbulent Shear Layers," J. Fluid Mechanics, Vol. 9, 1-28, (1960).

4. Lassiter, L.W., and Hubbard, H.H., "Experimental Studies of Noise from Subsonic Jets in Still Air," NACA TN-2757, (1952).

5. Ribner, H.S., "Reflection, Transmission and Amplification of Sound by a Moving Medium," J. Acoustical Society of America, Vol. 29, 435-441 (1957).

6. Miles, J.W., "On the Reflection of Sound at an Interface of Relative Motion," J. Acoustical Society of America, Vol. 29, 226-228 (1957).

7. Gottlieb, P., "Acoustics in Moving Media," Ph.D. Thesis, Physics Dept., Mass. Inst. of Tech. (1959), also "Sound Source Near a Velocity Discontinuity," J. Acoustical Society of America, Vol. 32, 1117-1122 (1960).

8. Moretti, G., and Slutsky, S., "The Noise Field of Subsonic Jets," General Applied Science Labs., GASL Tech. Rep. No. 150 (AFOSR TN-39-1310) (1959).

9. Slutsky, S., and Tamagno, J., "Sound Field Distribution about a Jet," General Applied Science Labs., GASL Tech. Rep. No. 259 (AFOSR TN 1935) (1961).

10. Slutsky, S., "Acoustic Field of A Cylindrical Jet Due to a Distribution of Random Sources or Quadrupoles," General Applied Science Labs., GASL Tech. Rep. No. 281 (1962).

11. Atvars, J., "Refraction of Sound by a Jet Velocity Field," M.A.Sc. Thesis, Univ. of Toronto, Inst. for Aerospace Studies (1964).

12. Schubert, L.K., "The Role of Jet Temperature and Sound Source Position in Refraction of Sound from a Point Source Placed in an Air Jet," M.A.Sc. Thesis, Univ. of Toronto, Inst. for Aerospace Studies (1965).

13. Atvars, J., Schubert, L.K., and Ribner, H.S., "Refraction of Sound from a Point Source Placed in an Air Jet," J. Acoustical Society of America, Vol. 37, No. 1, 168-170 (1965).

REFERENCES (Continued)

14. Atvars, J., Schubert, L.K., and Ribner, H.S., "Refraction of Sound from a Point Source Placed in an Air Jet," AIAA Paper No. 65-82, AIAA 2nd Aerospace Science Meeting, New York, Jan. 25-27, 1965.

15. Atvars, J., Schubert, L.K., Grande, E., and Ribner, H.S., "Refraction of Sound by Jet Flow and Jet Temperature," University of Toronto, Inst. for Aerospace Studies, UTIAS Technical Note No. 109 (May 1965).

16. Grande, E., "Refraction of Sound by Jet Flow and Jet Temperature, II," Univ. of Toronto, Inst. for Space Studies, UTIAS Technical Note No. 110, (1966).

17. Muller, E.A., and Matschat, K.R., "The Scattering of Sound by a Single Vortex and by Turbulence," U.S. Air Force Office of Scientific Research, AFOSR-TN-59-337, (January 1959).

18. Schmidt, D.W., "Experiments Relating to the Interaction of Sound and Turbulence," U.S. Air Force Office of Scientific Research, AFOSR-TN-60-357 (1959).

19. Ffowcs-Williams, J.E., "Some Thoughts on the Effects of Aircraft Motion and Eddy Convection on the Noise from Air Jets," University of Southampton, Aero/Astro Report No. 155, (1960).

20. Powell, A., "On the Generation of Noise by Turbulent Jets," American Society of Mechanical Engineers, ASME Paper 59-AV-53 (1959).

21. Ribner, H.S., "The Generation of Sound by Turbulent Jets," Advances in Applied Mechanics, Vol. 8, Academic Press, New York, 103-182 (1964).

22. Davies, P.O.A.L., Barratt, M.J., and Fisher, M.J., "Turbulence in the Mixing Region of a Round Jet," ARC 23, 728-N200-FM 3181 (1962).

23. Ffowcs-Williams, J.E., "The Noise from Turbulence Convected at High Speed," Philosophical Transactions, Royal Society of London, Series A, Vol. 255, 469-502, (1953).

24. Kraichnan, R.H., "The Scattering of Sound in a Turbulent Medium," J. Acoustical Society of America, Vol. 25, 1096-1104 (1953).

25. Shapiro, A.H., "The Dynamics and Thermodynamics of Compressible Fluid Flow," Vol. I and II, The Ronald Press, New York, (1953).

26. Lighthill, M.J., The Bakerian Lecture, 1961. "Sound Generated Aerodynamically," Proceedings of the Royal Society, Series A, Vol. 267, 147-182 (1962).

REFERENCES (Continued)

27. Lighthill, M.J., "On the Energy Scattered from the Interaction of Turbulence with Sound or Shock Waves," Proceedings of Cambridge Philosophical Society, Vol. 49, 531-551, (1953).

28. Lilley, G.M., "On the Noise from Air Jets," Aeronautical Research Council, ARC 20, 376-N40-rM 2724 (1958).

29. Powell, A., "Survey of Experiments on Jet Noise," Aircraft Engineering, Vol. 26, 2-9 (1954).

30. Jones, I.S.F., "Aerodynamic Noise Dependent on Mean Shear," J. Fluid Mechanics, Vol. 33, 65-73, (1968).

31. Ribner, H.S., "Aerodynamic Sound from Fluid Dilatations - A Theory of Sound from Jets and Other Flows," University of Toronto, Inst. for Aerospace Studies, UTIAS Rep. 86 (AFOSR TN 3430), (1962).

32. Ribner, H.S., "On Spectra and Directivity of Jet Noise," J. Acoustical Society of America, Vol. 35, No. 4, 614-616, (1963).

33. Davies, P.O.A.L., Fisher, M.J., and Barratt, M.J., "The Characteristics of the Turbulence in the Mixing Region of a Round Jet," J. Fluid Mechanics, Vol. 15, 337-367 (1963).

34. Wills, J.A.B., "On Convection Velocity in Turbulent Shear Flows," J. Fluid Mechanics, Vol. 20, p. 417 (1964).

35. Fisher, M.J., and Davies, P.O.A.L., "Correlation Measurement in a Non-Frozen Pattern of Turbulence," J. Fluid Mechanics, Vol. 18, 97-116 (1964).

36. Batchelor, G.K., "The Theory of Homogeneous Turbulence," Cambridge University Press, Cambridge (1960).

37. Potter, R.C., "An Investigation to Locate the Acoustic Sources in a High Speed Jet Exhaust Stream," Wyle Laboratories, Technical Report WR 68-4, (1968).

38. Margiarotty, R.A., Cuadra, D.E., Bowie, G.E., Large, J.B., Holman, F.S., "Acoustic and Thrust Characteristics of the Subsonic Jet Efflux from Model Scale Sound Suppressors," Part I, "Unheated Jets," The Boeing Company, Report No. D6-15071, Vol. II, (1966).

39. Mollo-Christensen, E., "Jet Noise and Shear Flow Instability Seen from an Experimenter's Viewpoint," Journal of Applied Mechanics, Vol. 34, 1-7, (1967).

REFERENCES (Continued)

40. Chu, W.T., "Turbulence Measurements Relevant to Jet Noise," University of Toronto, Inst. for Space Studies, UTIAS Report No. 119, (1966).

41. Jones, I.S.F., "Model for Prediction of Jet Noise from Measurements of Fluctuating Turbulence Stresses," Department of Mechanical Engineering, Univ. of Waterloo, Research Report No. 5 (1967).

42. Bendat, J.S., "Principles and Applications of Random Noise Theory," John Wiley, New York, (1958).

43. Grenander, U., and Rosenblatt, M., "Statistical Analysis of Stationary Time Series," John Wiley, New York, (1957).

44. Parzen, E., "Stochastic Processes," Holden-Day, San Francisco, (1962).

45. Parzen, E., "Modern Probability Theory and Its Applications," John Wiley, New York, (1960).

46. Jones, D.S., "Generalised Functions," McGraw-Hill, New York, (1966).

47. Uberoi, M.S., and Kovasznay, L.S.G., "On Mapping and Measurement of Random Fields," Quarterly Applied Mathematics, Vol. 10, 375-393, (1952).

48. Pe[illegible]A.C., and Cottrell, J.W., "Investigation to Define the Propagation Characteristics of a Finite Amplitude Acoustic Pressure Wave," NASA Contract Report CR-736, North American Aviation, Inc. (1967).

49. Bracewell, R.N., "Fourier Transforms and its Applications," McGraw Hill, New York, (1965).

50. Proudman, I., "The Generation of Noise by Isotropic Turbulence," Proceedings of Royal Soc. Ser. A., Vol. 214, pp. 119-132, (1952).

TABLE I

OCTAVE BANDWIDTH SPECIFICATION*

Octave Band Number (on Figures)	Band Lower Frequency Hz	Band Upper Frequency Hz	Band Center Frequency Hz
1	178	355	250
2	355	708	500
3	708	1410	1000
4	1410	2820	2000
5	2820	5620	4000
6	5620	11.2 kc	8000
7	11.2 kc	22.4 kc	16 kc
8	22.4 kc	44.6 kc	32 kc
9	44.6 kc	89.1 kc	64 kc

*These octave bands are chosen as the same as given in Reference 38.

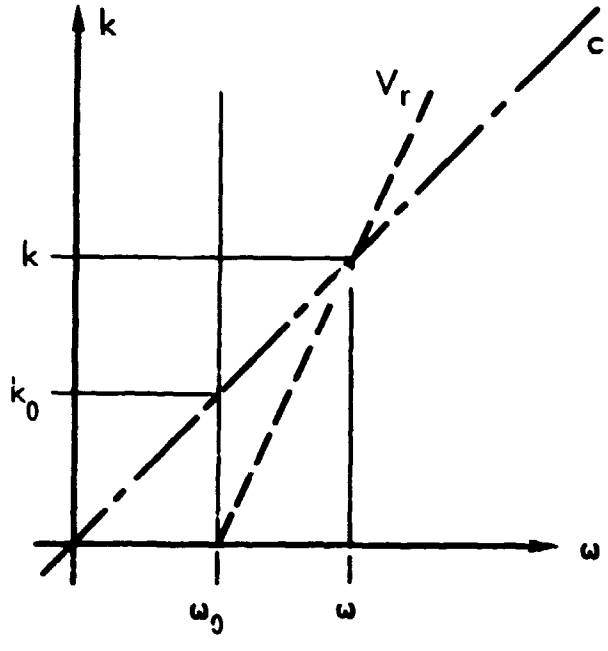

Figure 1. Location of Sound Radiating Element of a Moving Source in the Wave-Number Frequency Space: Subsonic Case

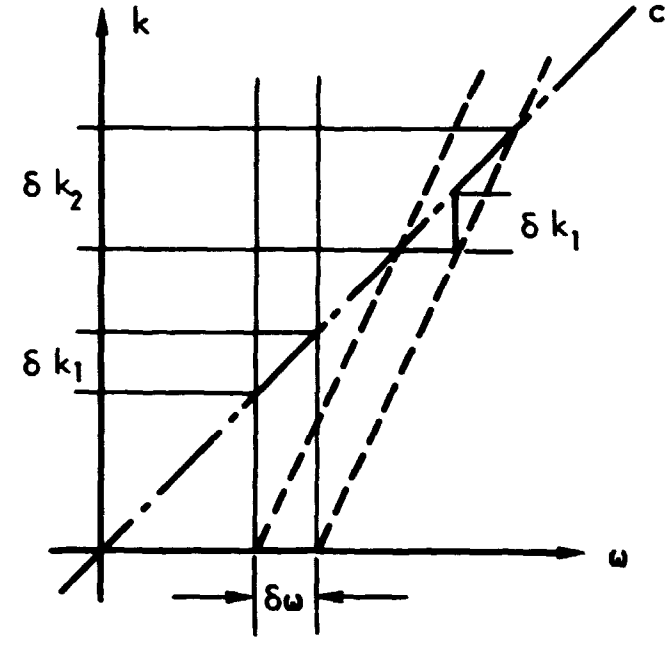

Figure 2. Enlargement of Figure 1.

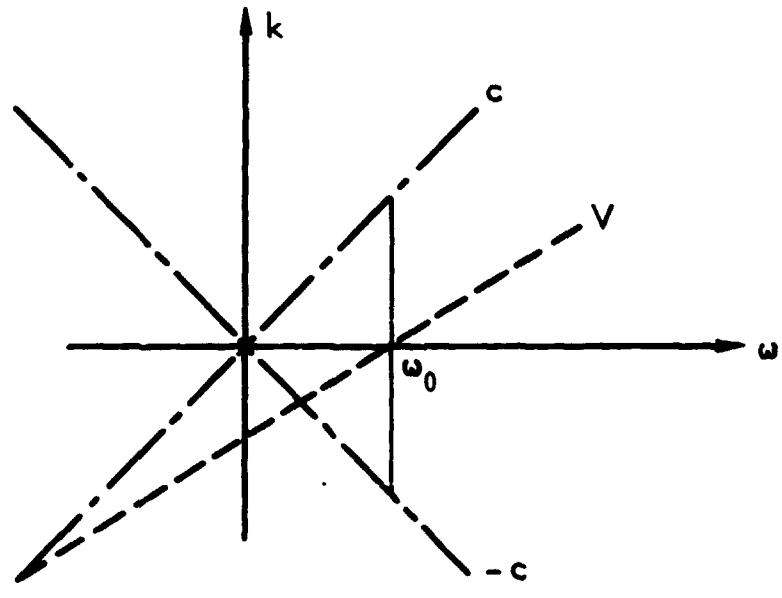

Figure 3. Location of Sound Radiating Element of a Moving Source in the Wave-Number Frequency Space: Supersonic Case

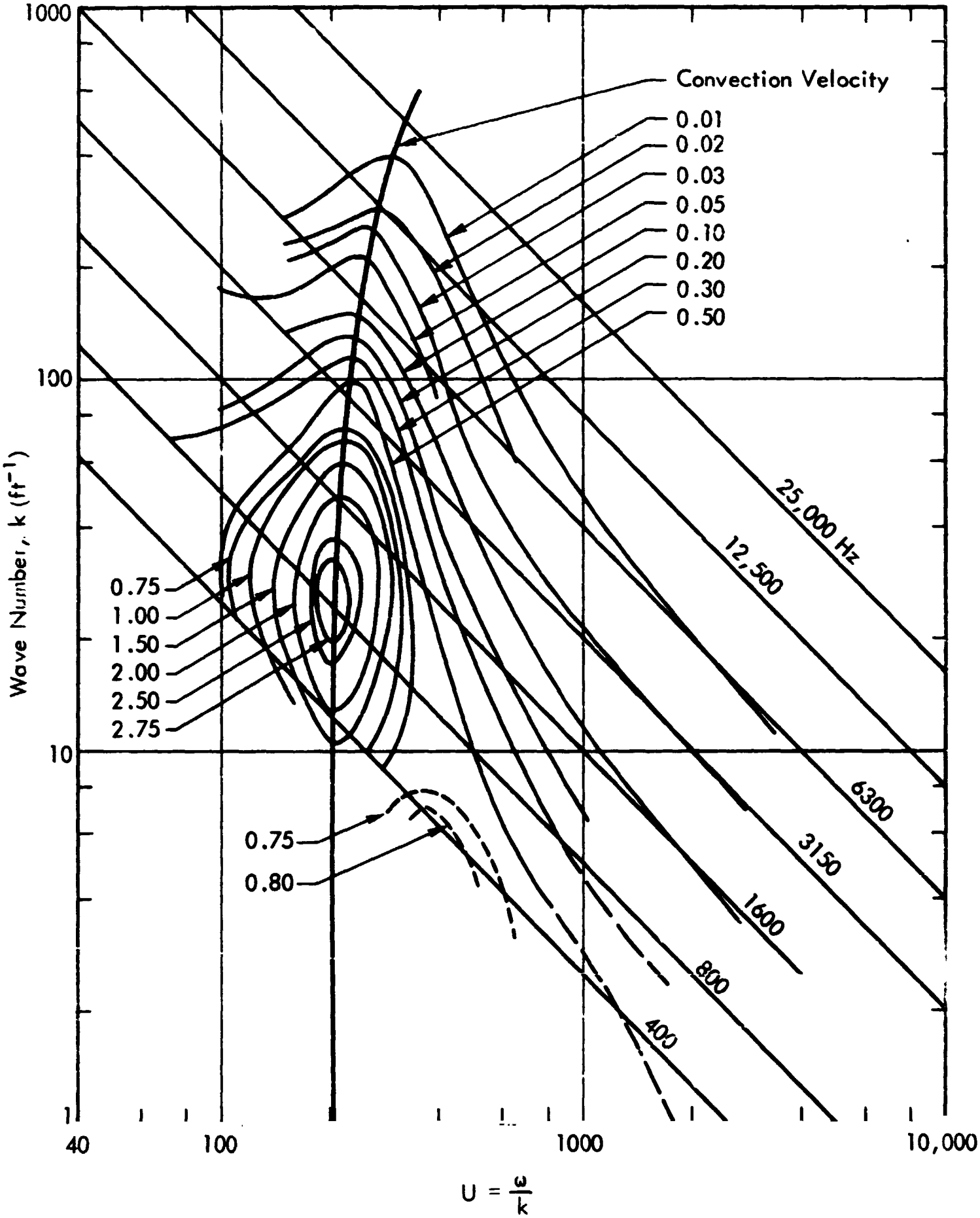

Figure 4. One-Dimensional Wave-Number Phase Velocity Spectrum of the Longitudinal Fluctuating Velocity Component in the Mixing Region of a Round Jet. (From Reference 34 as replotted to double logarithmic scales.)

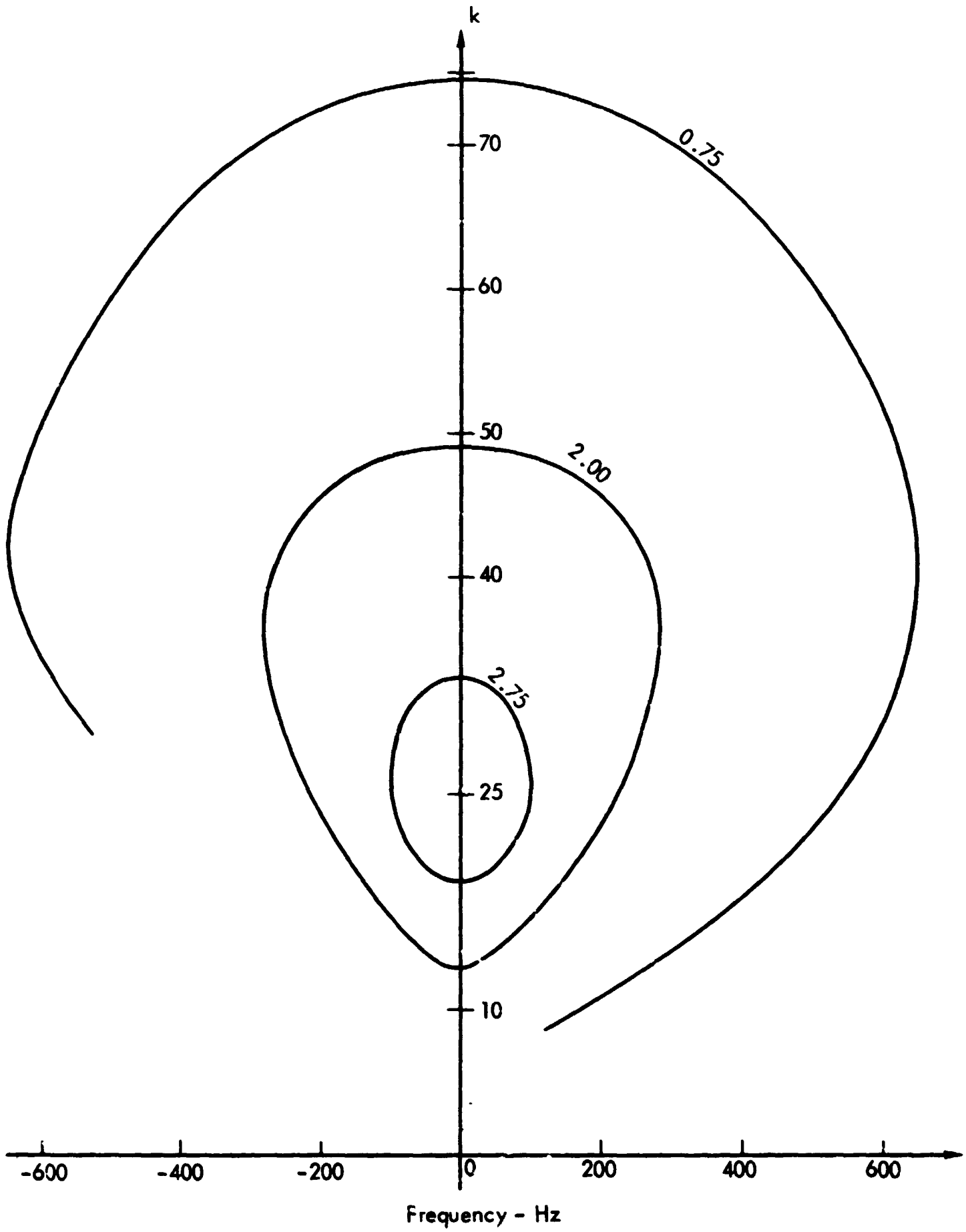

Figure 5. One-Dimensional Wave Number Frequency Spectrum In a Moving Frame of Reference

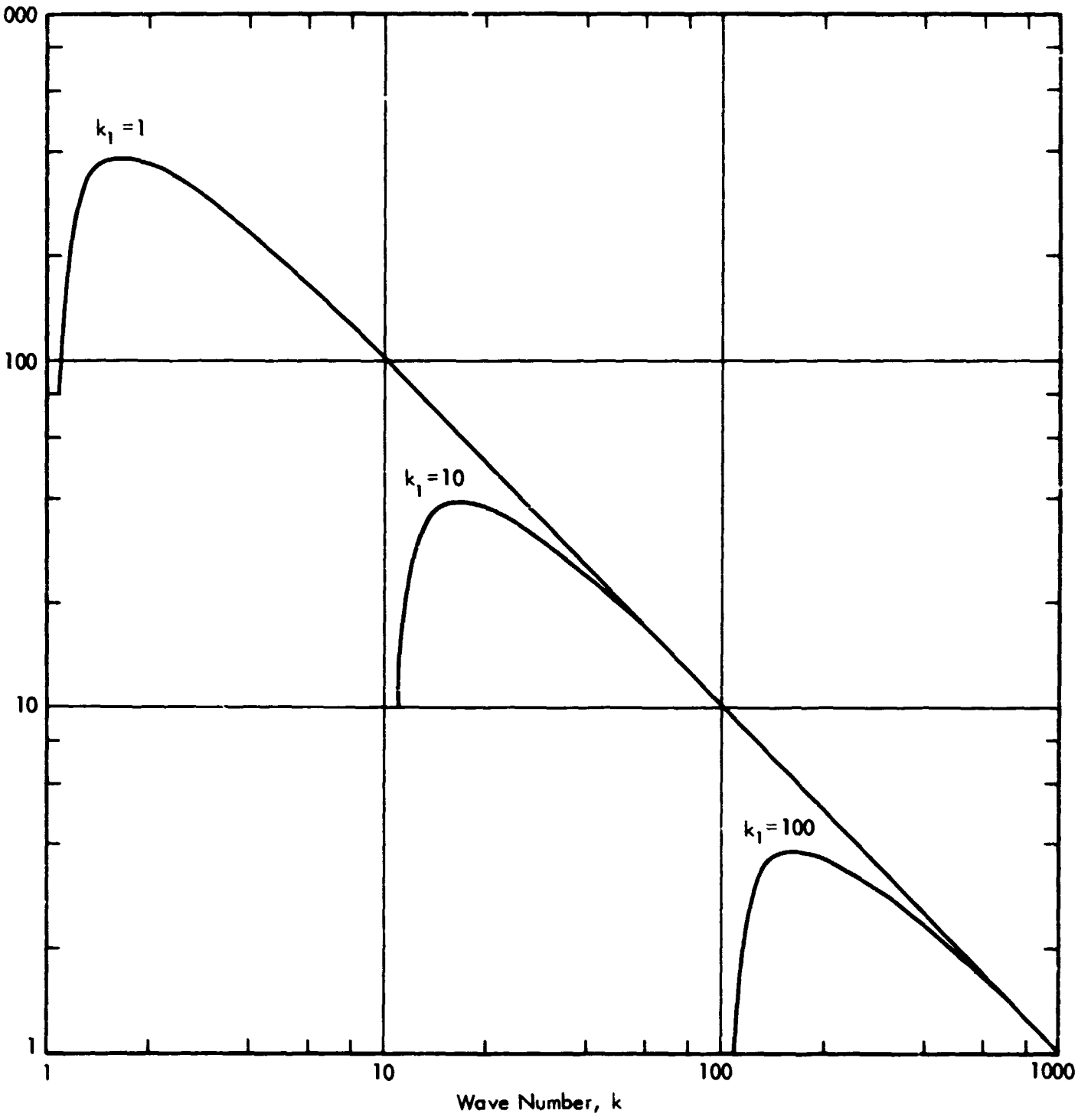

Figure 6. Values of the Integration Factor, $(1 - k_1^2/k^2)\ 1/k$, for Converting E(k) to $\phi_1(k)$

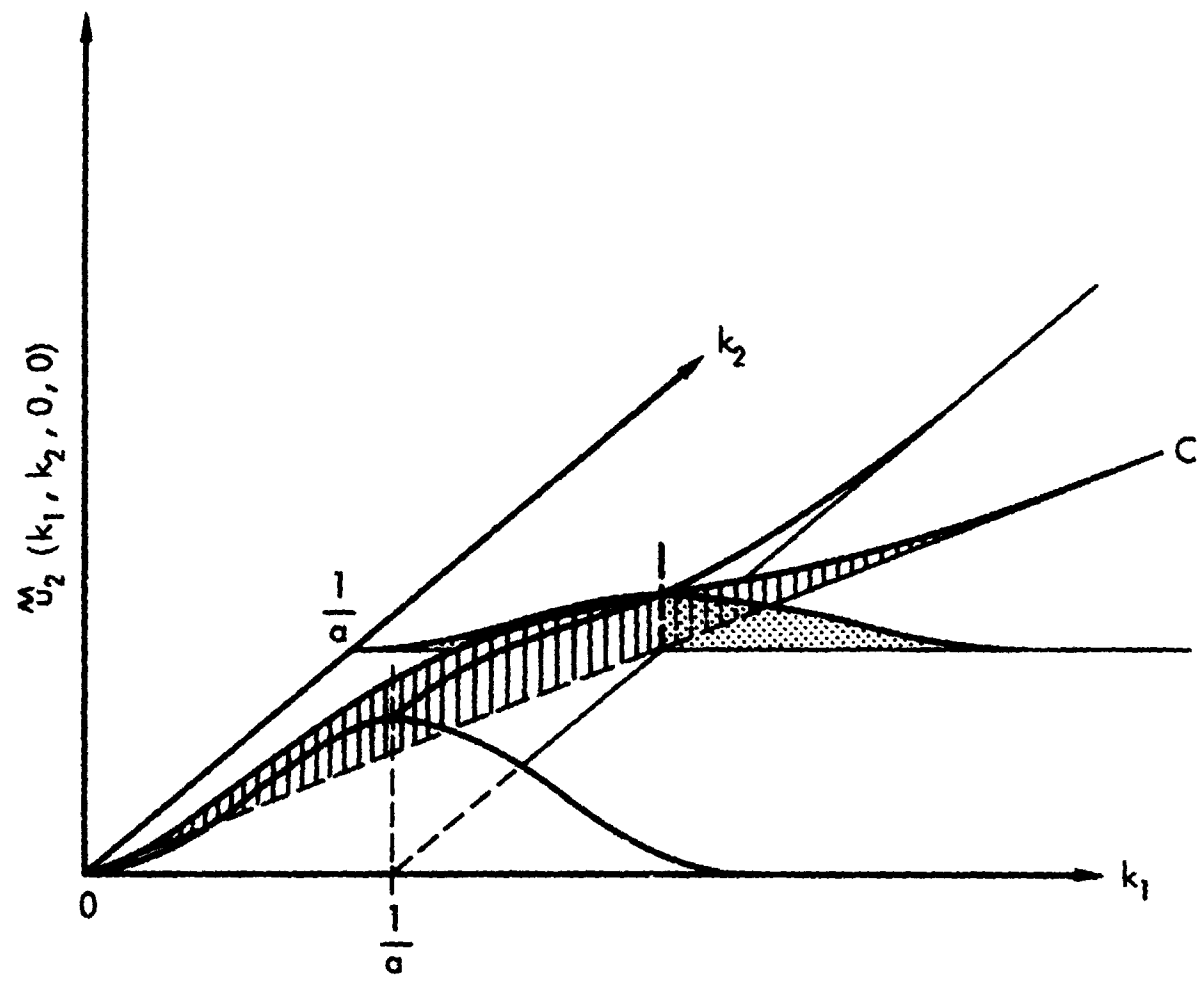

Figure 7. Distribution of Spectral Intensity of $\hat{\mathcal{U}}_2(\underset{\sim}{k}, \omega)$ in the k_1, k_2 Plane

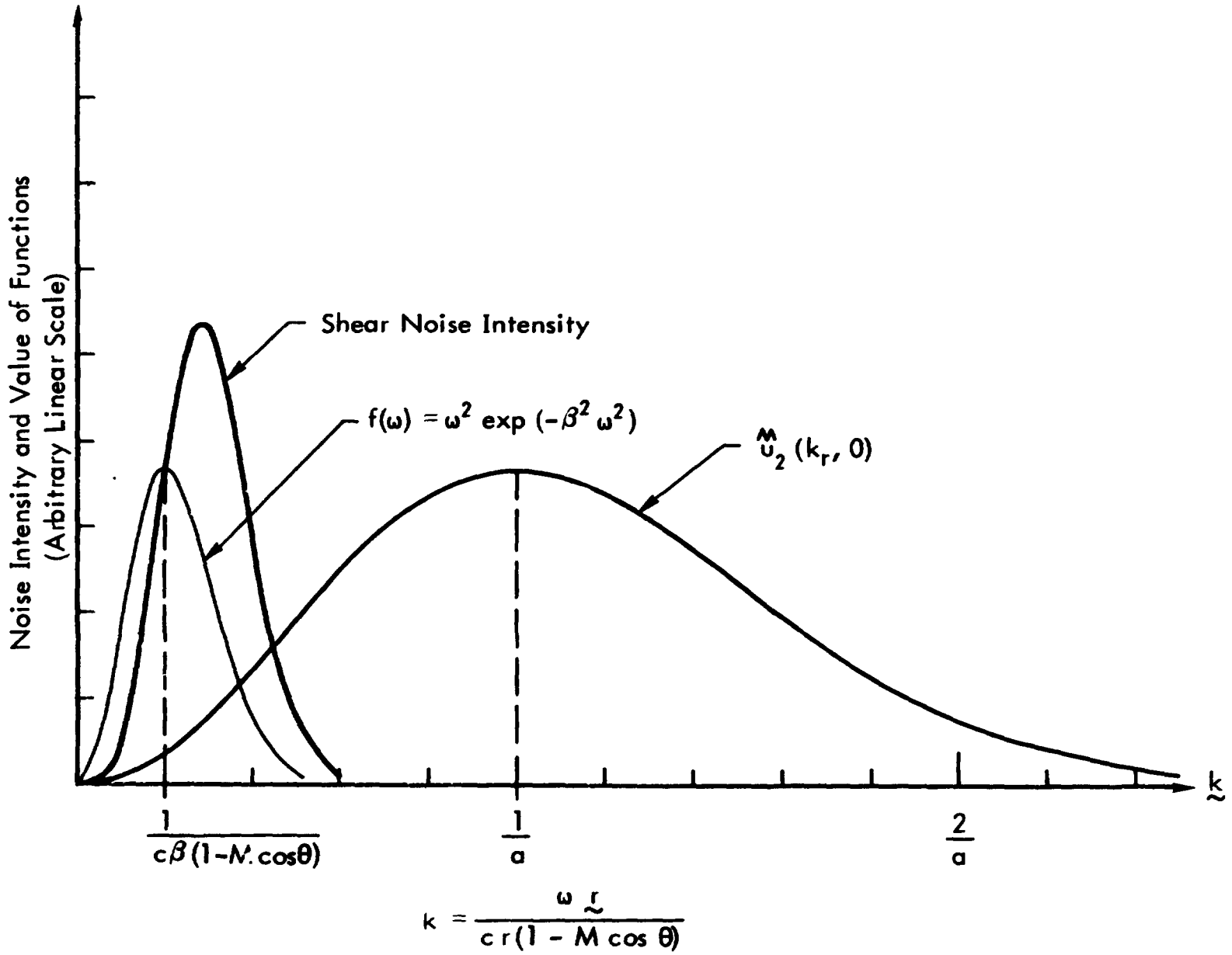

Figure 8. Location of the Peak Shear Noise Production Region on the Wave-Number Axis.

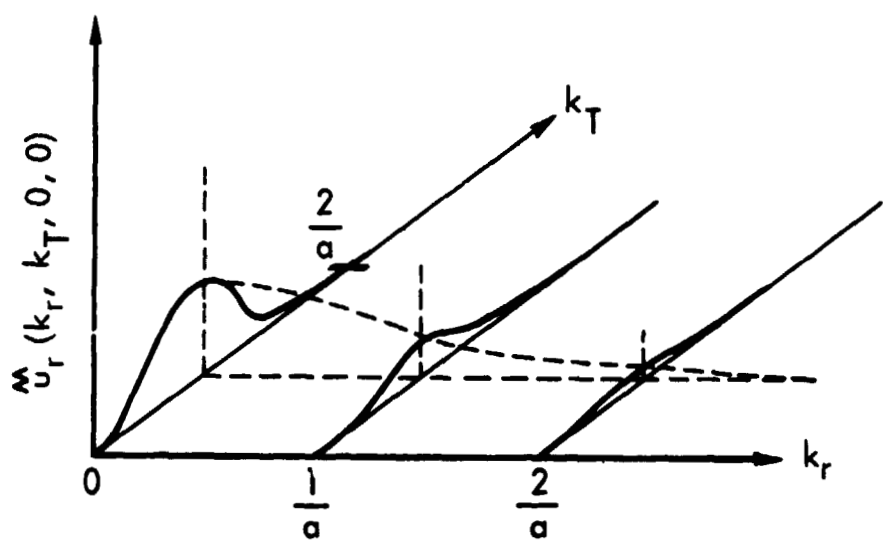

The Second Order Turbulence Spectrum $\hat{M}_{u_r}(\underset{\sim}{k}, \omega)$

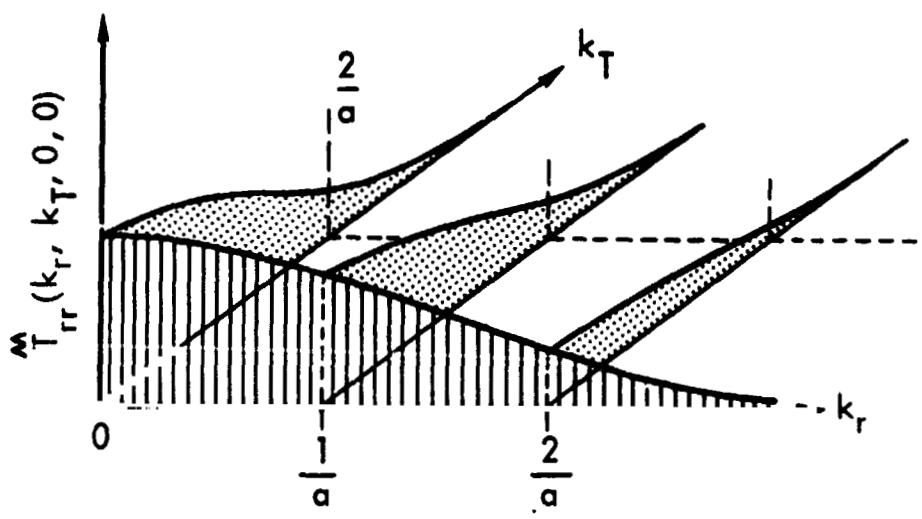

The Fourth Order Turbulence Spectrum $\hat{M}_{\Gamma_{rr}}(\underset{\sim}{k}, \omega)$

Figure 9. The Second Order and the Fourth Order Turbulence Spectral Intensity Distributions in the k_r, k_T Plane

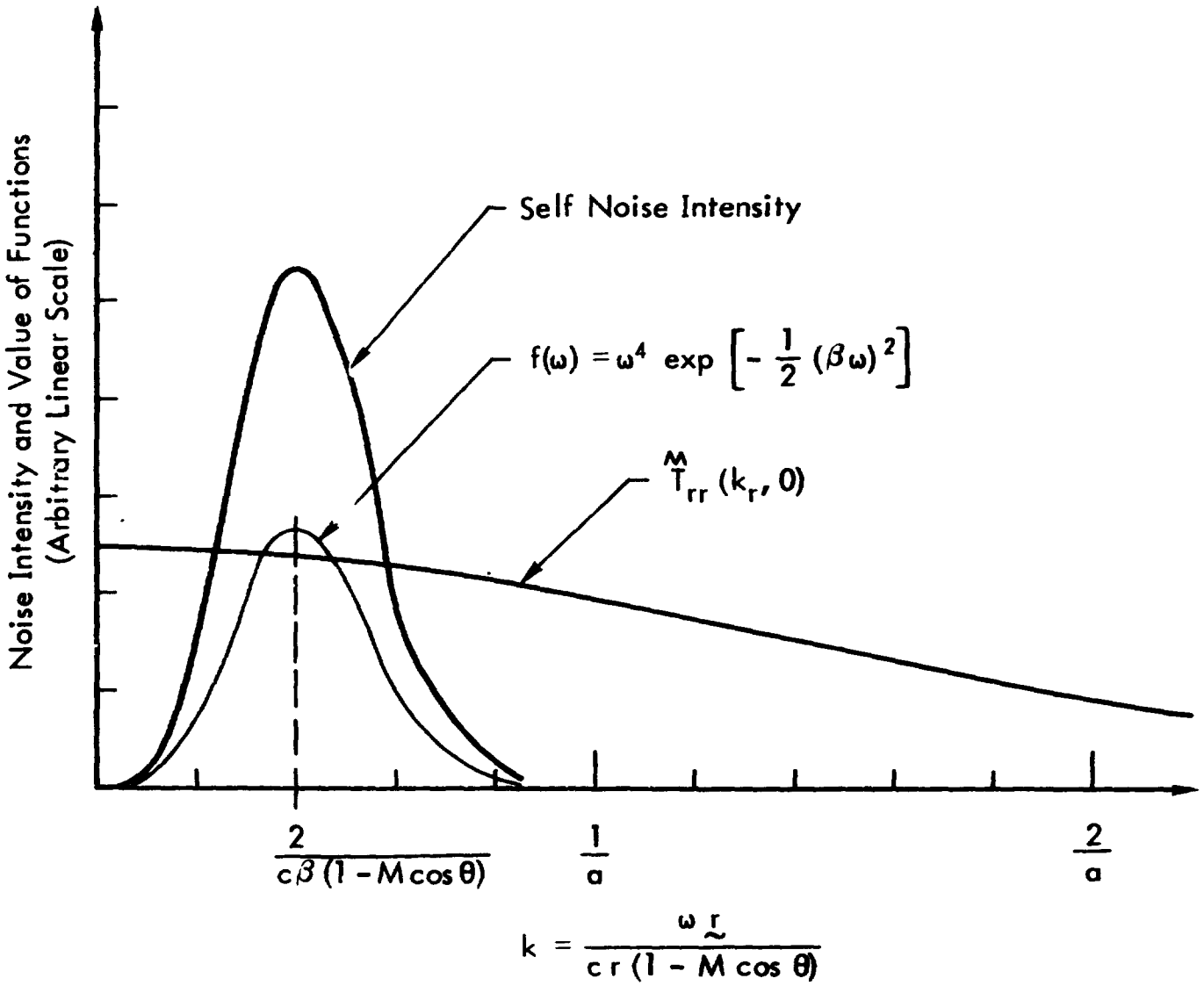

Figure 10. Location of the Peak Self Noise Production Region on the Wave Number Axis

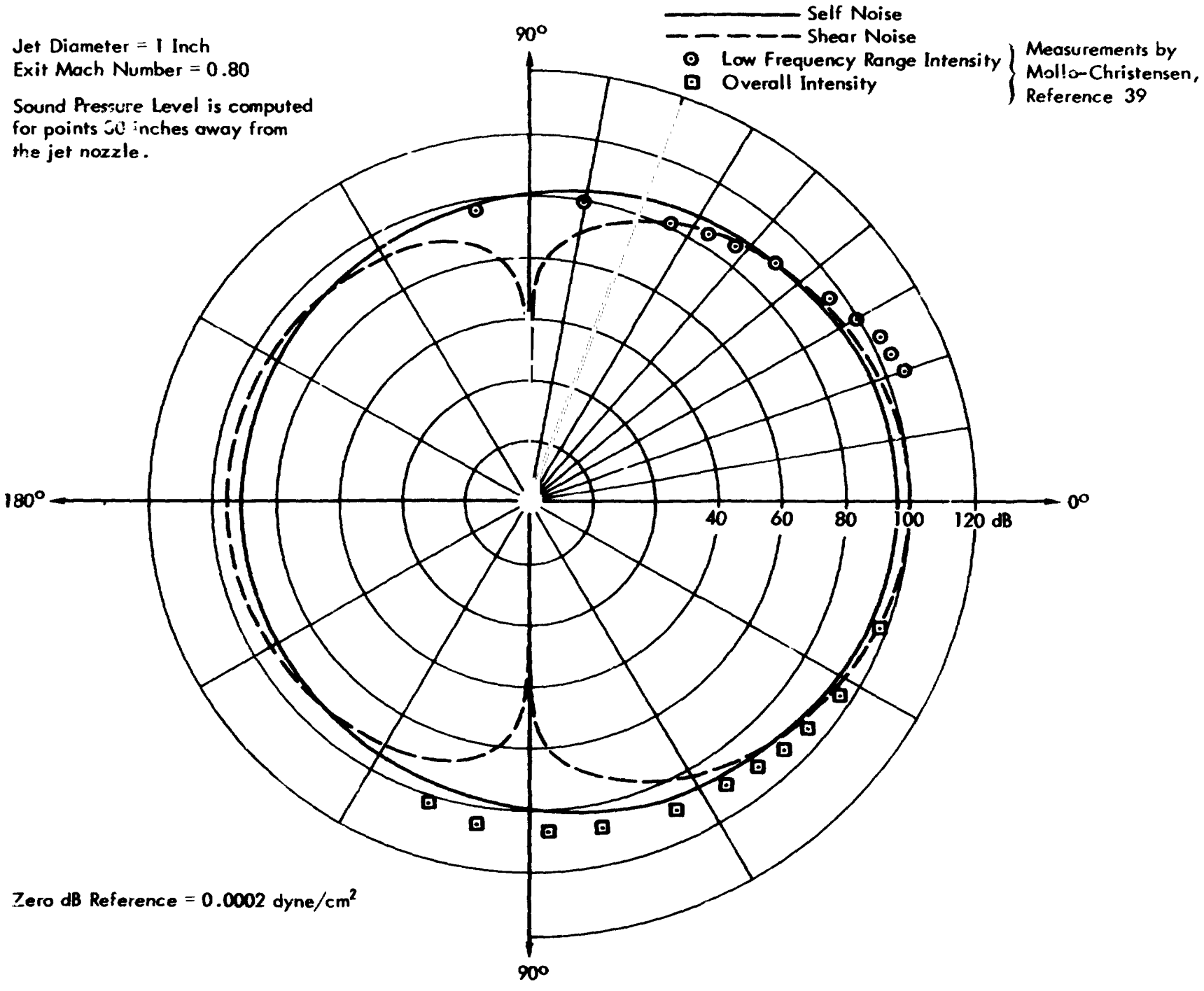

Figure 11. Comparison of Theoretical Jet Noise Prediction with Experimental Measurements by Mollo-Christensen (Reference 39)

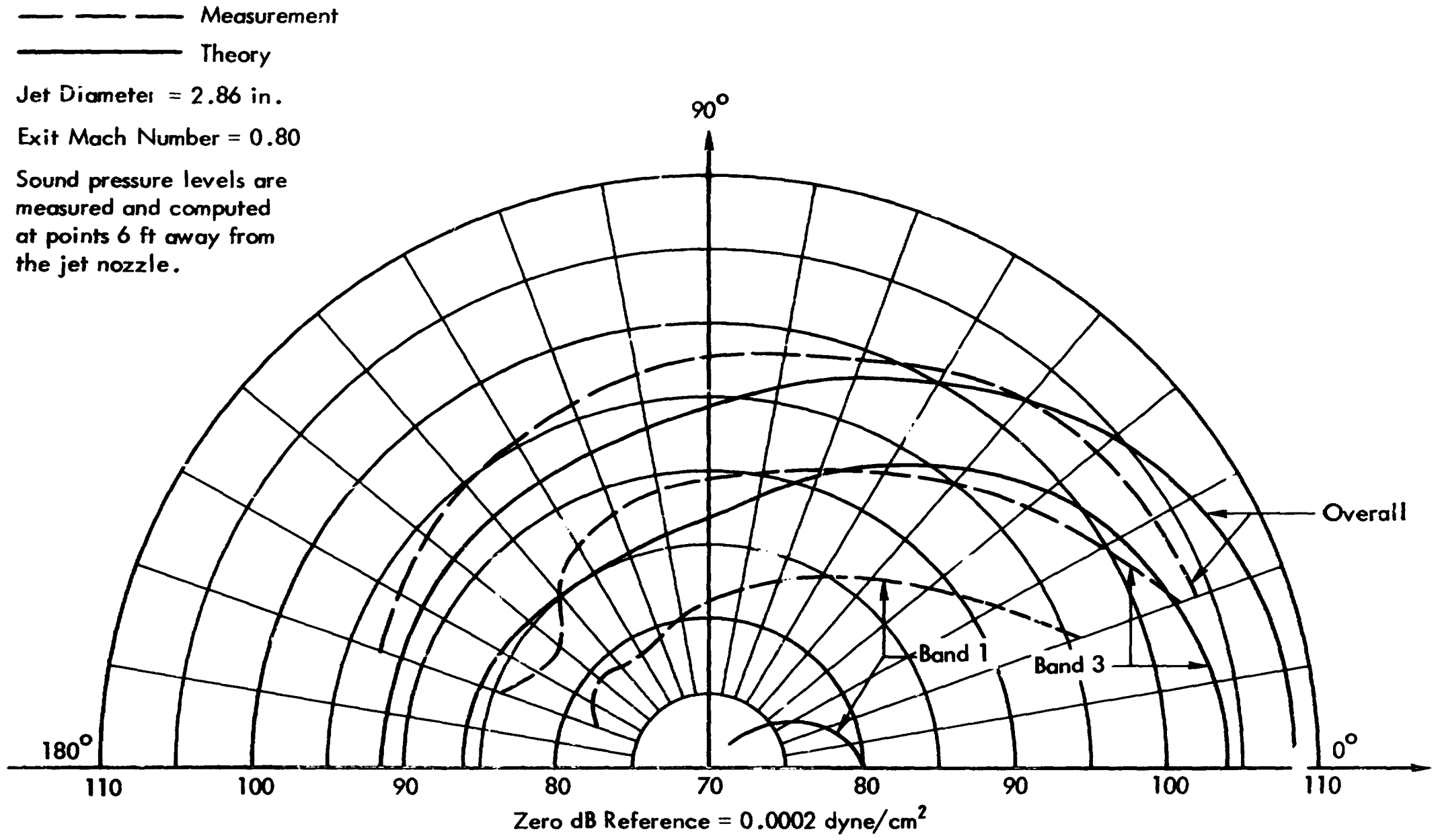

Figure 12. Comparison of Theoretical Jet Noise Prediction with Experimental Measurements by Mangiarotty et al. (Reference 38). Overall Noise and Octave Bands 1 and 3.

— — — — Measurement

———— Theory

Jet Diameter = 2.86 in.

Exit Mach Number = 0.80

Sound pressure levels are measured and computed at points 6 ft away from the jet nozzle.

Predicted noise levels for Band 7 and Band 9 are below 50 dB. These curves are not shown in this figure.

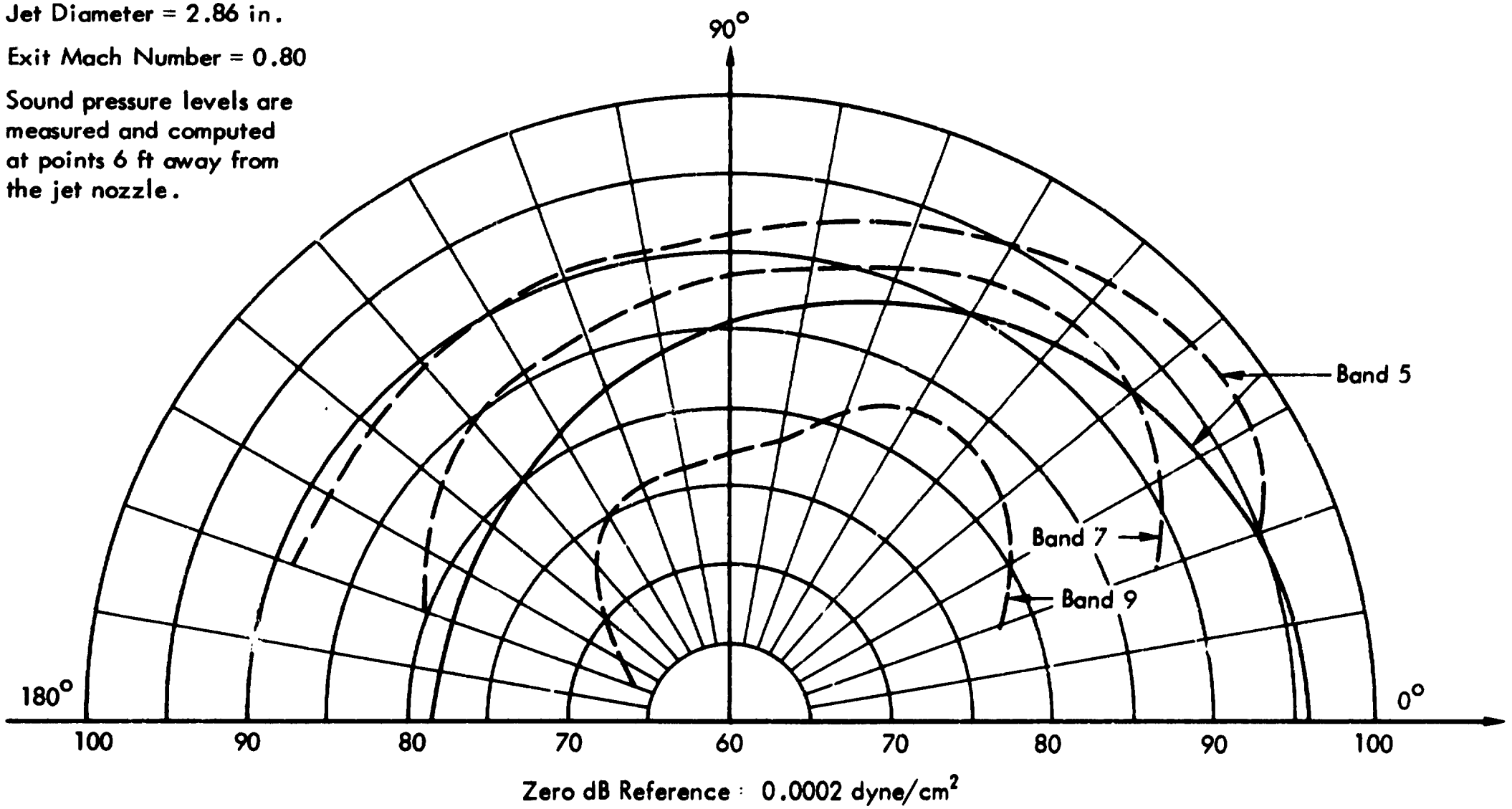

Figure 13. Comparison of Theoretical Jet Noise Prediction with Experimental Measurements by Mangiarotty et al. (Reference 38). Octave Bands 5, 7, and 9.

APPENDIX A

THREE-DIMENSIONAL SPECTRUM FUNCTIONS

A.1 Introduction

The notion of three- and four-dimensional spectrum functions is used extensively in the present report. One-dimensional spectra are widely familiar as a result of their use in the analysis of time varying phenomena, and the clarity and usefulness of the frequency spectrum of a time varying function is well known. Several books are available which treat one-dimensional spectra in detail (References 42-45). The three- or four-dimensional spectrum is a natural extension of the one-dimensional ideas. Here we are concerned with the spatial frequency, or wave number, representation of a spatially varying function. Since space has three dimensions, three wave-number components must be used to describe the complete wave spectrum. Analysis of a function into multi-dimensional spectra is a straightforward extension of the one-dimensional case, but because of its comparative unfamiliarity it has been thought worthwhile to include a fairly complete discussion here. The analysis below is restricted to three space dimensions, but the fourth, (time), dimension can readily be added, as was done in Section 4.0 of this report.

Several different forms for the basic Fourier decomposition are possible. The one used below, and in the body of the report has been used by several authors, and has the advantage that odd factors of 2π do not appear in the integrals.

Consider any function $u(\underset{\sim}{x})$. Then $\hat{u}(\underset{\sim}{k})$ the three-dimensional wave number spectrum of $u(\underset{\sim}{x})$ can be defined by

$$\hat{u}(k_1, k_2, k_3) = \int_{-\infty}^{+\infty}\int_{-\infty}^{+\infty}\int_{-\infty}^{+\infty} u(x_1, x_2, x_3) \exp - 2\pi i (k_1 x_1 + k_2 x_2 + k_3 x_3)\, dx_1\, dx_2\, dx_3 \qquad (A1)$$

Thus it can be seen that the three-dimensional wave spectrum of u is simply the multiple of three one-dimensional Fourier integrals, one for each dimension. The extension to additional dimensions is obvious. It is also clear that the Fourier inversion theorem may be applied to each one-dimensional integral separately. Equation (A1) and its inverse may be written in shorter form as

$$\hat{u}(\underset{\sim}{k}) = \int u(\underset{\sim}{x}) \exp - 2\pi i \, (\underset{\sim}{k} \cdot \underset{\sim}{x}) \, d\underset{\sim}{x} \tag{A2}$$

$$u(\underset{\sim}{x}) = \int \hat{u}(\underset{\sim}{k}) \exp 2\pi i \, (\underset{\sim}{k} \cdot \underset{\sim}{x}) \, d\underset{\sim}{x} \tag{A3}$$

Two points should be noted about Equations (A2), and (A3). The integrals are basically over all space. Therefore, u, $\hat{u}$ must tend to zero sufficiently rapidly at infinity to allow the integral to converge. Thus, homogeneous (e.g., random) functions, which do not tend to zero at infinity must be specially analyzed, as in Section A.3 below. Note particularly that $\hat{u}(\underset{\sim}{k})$ is an integral representation of the entire function $u(\underset{\sim}{x})$. No details of localized spatial structure appear, and the wave spectrum $u(\underset{\sim}{k})$ may be assumed to apply uniformly over the whole $\underset{\sim}{x}$ space.

A.2 Convolution Product

The spectral form of the multiple of two functions is used extensively in the report (Section 5), and will also be required below. To simplify the understanding of the proof of the relations, consider first the vector quantities below as scalars. The proof applies directly for scalars, and the steps may then readily be extended to the vector form.

$$\text{Let} \qquad u(\underset{\sim}{x}) = v(\underset{\sim}{x}) \, w(\underset{\sim}{x}) \tag{A4}$$

$$\text{By (A2)} \qquad \hat{u}(\underset{\sim}{k}) = \int v(\underset{\sim}{x}) \, w(\underset{\sim}{x}) \exp -(2\pi i \, k\underset{\sim}{x}) d\underset{\sim}{x}$$

Now introduce the spectrum function $v(\underset{\sim}{\ell})$ of $v(x)$ in a relation as (A3)

$$\hat{u}(\underset{\sim}{k}) = \int_{\underset{\sim}{x}} \int_{\underset{\sim}{\ell}} \hat{v}(\underset{\sim}{\ell}) \exp(2\pi i \, \ell\underset{\sim}{x}) w(\underset{\sim}{x}) \exp(-2\pi i \underset{\sim}{k} \cdot \underset{\sim}{x}) \, d\underset{\sim}{x} \, d\underset{\sim}{\ell}$$

$$= \int_{\underset{\sim}{\ell}} \hat{v}(\underset{\sim}{\ell}) \int_{\underset{\sim}{x}} w(\underset{\sim}{x}) \exp\left\{- 2\pi i \, (\underset{\sim}{k} - \underset{\sim}{\ell}) \cdot \underset{\sim}{x}\right\} d\underset{\sim}{x} \, d\underset{\sim}{\ell} \tag{A5}$$

The $\underset{\sim}{x}$ integral may be identified as $\hat{w}(\underset{\sim}{k} - \underset{\sim}{\ell})$ via (A2) so that Equation (A5) may be written

$$\hat{u}(\underset{\sim}{k}) = \int_{\underset{\sim}{\ell}} \hat{v}(\underset{\sim}{\ell})\, \hat{w}(\underset{\sim}{k} - \underset{\sim}{\ell})\, d\underset{\sim}{\ell} \tag{A6}$$

Expression (A6) is known as the Convolution Product of the spectral functions. A short notation in wide use for convolution products is

$$\hat{u}(\underset{\sim}{k}) * \hat{w}(\underset{\sim}{k}) = \int_{\underset{\sim}{\ell}} \hat{v}(\underset{\sim}{\ell})\, \hat{w}(\underset{\sim}{k} - \underset{\sim}{\ell})\, d\underset{\sim}{\ell} \tag{A7}$$

The above analysis shows that when the space function is the product of two space functions the spectrum is the convolution product of their spectra. Thus

$$\left.\begin{aligned} &\text{when} \quad u(\underset{\sim}{x}) = v(\underset{\sim}{x})\, w(\underset{\sim}{x}) \\ &\text{then} \quad \hat{u}(\underset{\sim}{k}) = \hat{v}(\underset{\sim}{k}) * \hat{w}(\underset{\sim}{k}) \end{aligned}\right\} \tag{A8}$$

An inverse relation also applies, and may be proved directly by the same methods as above. It is

$$\left.\begin{aligned} &\text{when} \quad \hat{u}(\underset{\sim}{k}) = \hat{v}(\underset{\sim}{k})\, \hat{w}(\underset{\sim}{k}) \\ &\text{then} \quad u(\underset{\sim}{x}) = v(\underset{\sim}{x}) * w(\underset{\sim}{x}) \end{aligned}\right\} \tag{A9}$$

These convolution relations (A8) and (A9) have very wide application, as shown in Section 4 of this report, and in the next two sections below.

A.3 Random Functions

If $u(x)$ is now assumed to be a random function of space then it will not satisfy the limits at infinity required for the Fourier integration. In principle this raises considerable problems of mathematical rigor. However, it is possible to treat the integral as a form of "Generalized Function". Jones (Reference 46) has given an extensive development of the mathematics necessary in this case, which essentially shows that all common mathematical manipulations of the infinite integral are possible.

Now the random variable $u(x)$ will cancel out identically a Fourier integration over all space, except for $k = 0$. The fluctuating quantities have zero mean, by

definition. Thus the function $u(k)$ has a rather nebulous meaning. But the square of the random variable will have contributions at all wave numbers. To find this define a function $u_V(x)$ which exists only inside a limited volume V, and define therefore

$$\hat{u}_V(\underset{\sim}{k}) = \int u_V(\underset{\sim}{x}) \exp - 2\pi i \, \underset{\sim}{k} \cdot \underset{\sim}{x} \, dx \tag{A10}$$

The mean square value of $\hat{u}_V(\underset{\sim}{k})$ can now be defined as

$$\overset{\wedge\wedge}{u}(\underset{\sim}{k}) = \underset{V \to \infty}{\text{Limit}} \frac{1}{V} \left| \hat{u}_V(\underset{\sim}{k}) \, \hat{u}^*_V(\underset{\sim}{k}) \right| \tag{A11}$$

where the * superscript denotes a complex conjugate. $\overset{\wedge\wedge}{u}$ is thus a second order spectrum. From (A10) it is clear that $u^*_V(k) = u_V(-k)$, so that using relations (A9) the Fourier Transform of $u(k)$ can be defined as

$$\overline{u(\underset{\sim}{\xi})} = \underset{V \to \infty}{\text{Limit}} \frac{1}{V} \left| u_V(\xi)_* \; u_V(-\xi) \right| \tag{A12}$$

or, in the longer form

$$\overline{u(\underset{\sim}{\xi})} = \underset{V \to \infty}{\text{Limit}} \frac{1}{V} \int u_V(\underset{\sim}{x}) \, u_V(\underset{\sim}{x} - \underset{\sim}{\xi}) \, d\underset{\sim}{x} \tag{A13}$$

Equation A13 shows that $\overline{u(\xi)}$ is actually the cross correlation function of $u(x)$. $\overline{u(\underset{\sim}{\xi})}$ may readily be observed to be even in $\underset{\sim}{\xi}$ by substituting $\underset{\sim}{y} = \underset{\sim}{x} + \underset{\sim}{\xi}$ in (A13). The negative sign for $\underset{\sim}{\xi}$ can therefore be replaced by a positive sign if desired.

$\overline{u(\underset{\sim}{\xi})}$ is the three-dimensional correlation function. It is again an integral representation of the whole $u(\underset{\sim}{x})$ field, and is dependent only on the separation $\underset{\sim}{\xi}$. (Note that it would be meaningless to use the x variable in u). $\overset{\wedge\wedge}{u}(\underset{\sim}{k})$ is the wave number energy density spectrum, and is the Fourier Transform of correlation function, as is familiar from the one-dimensional case. Equation (A12) makes it clear that $\overset{\wedge\wedge}{u}(\underset{\sim}{k})$ is a mean square energy per unit volume. This fact is of importance when considering transformed coordinate systems, which may involve volumetric changes.

A.4 Three-Dimensional Transfer Functions

An important class of problems involve operations which can be described by

$$u(\underset{\sim}{x}) = \int h(\underset{\sim}{\xi})\, v(\underset{\sim}{x} - \underset{\sim}{\xi})\, d\underset{\sim}{\xi} \tag{A14}$$

ie. $u(\underset{\sim}{x}) = h(\underset{\sim}{x}) * v(\underset{\sim}{x})$

From Equation (A9) the spectral form is

$$\hat{u}(\underset{\sim}{k}) = \hat{h}(\underset{\sim}{k})\, \hat{v}(\underset{\sim}{k}) \tag{A15}$$

and thus the energy density spectrum is clearly

$$\hat{\hat{u}}(\underset{\sim}{k}) = \underset{V\to\infty}{\text{Limit}} \left\{ \frac{\hat{u}_{V}(\underset{\sim}{k})\, \hat{u}^{*}_{V}(\underset{\sim}{k})}{V} \right\} = \hat{\hat{h}}(\underset{\sim}{k})\, \hat{\hat{v}}(\underset{\sim}{k}) \tag{A16}$$

Thus for this transfer function problem the spectrum is described particularly easily by simple multiplication of the power spectra of the input and transfer functions.

This case corresponds to the response of a constant parameter linear system, such as a body or an instrument, to the random variable v(x). This formulation was extensively used by Uberoi and Kovasznay (Reference 47) in their study of instrumentation effects in turbulence measurements. The formulation can be applied whenever the kernel function h is not a function of space. For instance the spectral response function of a hot-wire anemometer is not a function of location. Neither would the response of an aircraft to a turbulent environment be dependent on position. Thus, the transfer function approach does apply to a wide variety of problems and gives answers directly. But note that in this report the inhomogeneity of the jet is a function of position, and transfer function methods are not appropriate. Thus, Equations (A8) are used rather than the transfer Equations (A9). For this case a more complex formulation is required.

APPENDIX B

COMPUTING PROGRAM FOR THE MODEL JET NOISE PREDICTIONS

B.1 Listing of the Computing Program 3200 FORTRAN (2.2) / /

```
      PROGRAM NOISES
C
C **  CALCULATES THE FOLLOWING ...
C **     . OCTAVE BAND LEVEL NOISE
C **        , SHEAR = DB
C **        , SELF  = DB
C **        , TOTAL = DB
C **
C **     . OVERALL NOISE
C **        , SHEAR = DB
C **        , SELF  = DB
C **        , TOTAL = DB
C **
C **     . OVERALL POWER
C **        , SHEAR = WATTS
C **        , SELF  = WATTS
C **        , TOTAL = WATTS
C **
C
      DIMENSION SHER(11), SELF(11), TOT(11), KITLE(20), Y(65), Z(65)
      DIMENSION KATE(2), U(181), V(181), W(10)
C
      LOOP = 0
      PI = 3.1415927
      CTR = 0.017453292
      RTD = 57.295779
      PI2 = PI * PI
      H = 0.011046875
      WATT = 1.35582
      SMALL = 1. / ( 1.E+12 )
C
      READ(60,500) (KATE(J),J=1,2)
C
   10 READ(60,500) (KITLE(J),J=1,20)
      IF( KITLE(1) .EQ. 4HEND )  499,20
C
   20 READ(60,502) SA, RHO, PARTIAL, SU, SC, SR
      READ(60,502) BIGM, ALPHA, WN, BIGD
C
      BETA = SA / ( ALPHA * SC * BIGM )
      BIGV = 2.5 * PI * BIGD**3
C
      WRITE(61,530)
      WRITE(61,504) (KITLE(J),J=1,20), (KATE(J),J=1,2)
      WRITE(61,532) SA,RHO, PARTIAL,SU
      WRITE(61,534) SC,SR,BIGM,ALPHA
      WRITE(61,536) WN, BIGD, BETA, BIGV
      WRITE(61,506)
      WRITE(61,508)
C
      SA2 = SA * SA
      SA3 = SA * SA2
      SC3 = SC**3
      AM2 = ( ALPHA * BIGM )**2
      AC2 = SA2 / ( SC * SC )
      AM = 1. / AM2
      FOUR = ( SU * ALPHA * BIGM )**4
      SCR2 = ( SC * SR )**2
      SU2 = SU * SU
      TOP = 1.5 * SQRT(2.*PI) * FOUR * BIGV
```

```
      BOT = 128. * SA * SCR2
      P3 = ( TOP * RHO * PI ) / ( 64. * SA * SC )
      P3 = P3 * WATT
      C9 = TOP / BOT
      TOP = BIGV * PARTIAL * PARTIAL * 1.5 * SQRT(PI) * SA * FOUR
      BOT = 128. * PI2 * SCR2 * SU2
      P2 = ( TOP * RHO ) / ( 64. * PI * SC * SU2 )
      P2 = P2 * WATT
      C8 = TOP / BOT
      VA32 = ( BIGV * SA3 ) / 32.
      SQS = ( SA * SU * PARTIAL ) / ( PI * SR * SC3 )
      SQS = SQS * SQS
      C1 = VA32 * SQS * BETA
      D1 = BIGV * SA3 * BETA * SU**4
      D2 = 128. * ( SC3*SR )**2
      C2 = D1 / D2
      W(1) = WN
      DO 30 J = 2,10
   30 W(J) = 2. * W(J-1)
      WRITE(61,538) (W(J),J=1,10)
C
C **  BEGINNING OF THETA LOOP, **  THETA = 0 - 180 DEGREES IN
C     10 DEGREE INCREMENTS
C
      DO 200 KT = 10,190,10
      KTHETA = KT - 10
      THETA = DTR * FLOAT( KTHETA )
      CTHETA = COS( THETA )
      D1 = 1. + BIGM*CTHETA
      C3 = D1 * D1
      C4 = C3 * C3 * D1
      C6 = 1. / C3
      D2 = CTHETA * CTHETA
      TCOS = D2 + D2*D2
      C5 = C1 * TCOS / C4
      C6 = .4C2 * ( C6 + AM )
      C7 = 0.5 * C6
      C10 = C2 / C4
C
C **  BAND LEVEL COMPUTATION
C
      DO 150 KB = 1,10
      HW = H * W(KB)
      SW = 0.707*W(KB) - HW
C
      DO 110 KH = 1,65
      SW = SW + HW
      W1 = SW * SW
      W2 = W1 * W1
      Y(KH) = W2 * EXP( W1*C6 )
  110 Z(KH) = W2 * EXP( W1*C7 )
C
      YA = 0.
      YB = 0.
      YC = 0.
      ZA = 0.
      ZB = 0.
      ZC = 0.
C
      YA = Y(1) + Y(65)
      ZA = Z(1) + Z(65)
      DO 112 J = 2,64,2
```

```
      YB = Y(J) + YB
  112 ZB = Z(J) + ZB
      DO 114 J = 3,63,2
      YC = Y(J) + YC
  114 ZC = Z(J) + ZC
      YA = C5 * HW * ( YA + 4.*YB + 2.*YC ) / 3.
      ZA = C10 * HW * ( ZA + 4.*ZB + 2.*ZC ) / 3.
C
C
C     IF( ABS( YA ) .LE. SMALL )  121,120
  120 CHECK   127.6 + 10.*ALOG10( YA )
      IF( CHECK .LT. 0. )  121,122
  121 CHECK = 0.0
  122 SHER(KB) = CHECK
C
C     IF( ABS( ZA ) .LE. SMALL )  127,126
  126 CHECK = 127.6 + 10.*ALOG10( ZA )
      IF( CHECK .LT. 0. )  127,128
  127 CHECK = 0.0
  128 SELF(KB) = CHECK
C
C     IF( ABS( YA+ZA ) .LE. SMALL )  133,132
  132 CHECK = 127.6 + 10.*ALOG10( YA+ZA )
      IF( CHECK .LT. 0. )  133,134
  133 CHECK = 0.0
  134 TOT(KB) = CHECK
C
  150 CONTINUE
C
C
C **  OVERALL NOISE COMPUTATION
C
      BOT = ( C3 + AM2 )**(2.5)
      D1 = TCOS * C8 / BOT
      D2 = C9 / BOT
C
      SHER(11) = 127.6 + 10.*ALOG10( D1 )
      SELF(11) = 127.6 + 10.*ALOG10( D2 )
      TOT(11)  = 127.6 + 10.*ALOG10( D1+D2 )
C
C
      IF( LOOP .GT. 9 ) 160,170
C
  160 WRITE(61,530)
      WRITE(61,504) (KITLE(J),J=1,20), (KATE(J),J=1,2)
      WRITE(61,506)
      WRITE(61,508)
      WRITE(61,538) (W(J),J=1,10)
      LOOP = 0
C
  170 WRITE(61,510) KTHETA, (SHER(J),J=1,11)
      WRITE(61,512) (SELF(J),J=1,11)
      WRITE(61,514) (TOT(J),J=1,11)
      LOOP = LOOP + 1
C
  200 CONTINUE
C
C
C **  OVERALL POWER CALCULATION
C
      ONEDEG = DTR
      THETA = ONEDEG
```

```
      DO 310 J = 1,181
      THETA = THETA + ONEDEG
      T = COS( THETA )
      ST = SIN( THETA )
      T2 = T * T
      T4 = T2 * T2
      TM = ( 1. - BIGM*T )**2
      DUM = ST / ( TM * AM2 )**(2.5)
      U(J) = ( T4 + T2 ) * DUM
  310 V(J) = DUM
C
      UA = 0.
      UB = 0.
      UC = 0.
      VA = 0.
      VB = 0.
      VC = 0.
      UA = U(1) + U(181)
      VA = V(1) + V(181)
      DO 320 J = 2,180,2
      UB = U(J) + UB
  320 VB = V(J) + VB
      DO 330 J = 3,179,2
      UC = U(J) + UC
  330 VC = V(J) + VC
      UB = ONEDEG * ( UA + 4.*UB + 2.*UC ) / 3.
      VB = ONEDEG * ( VA + 4.*VB + 2.*VC ) / 3.
      UA = P2 * UB
      VA = P3 * VB
      TA = UA + VA
C
      WRITE(61,516)
      WRITE(61,518)
      WRITE(61,520) UA, UB
      WRITE(61,522) VA, VB
      WRITE(61,524) TA
C
      LOOP = 0
      GO TO 10
C
  495 WRITE(61,530)
C
C
C **  FORMAT STATEMENTS
C
  500 FORMAT( 20A4 )
  502 FORMAT( 6F10.0 )
  504 FORMAT( 10X,20A4,30X,2A4 // )
  506 FORMAT( 5X,5HTHETA,29X,57HO C T A V E    B A N D    L E V E L    N
     * O I S E    *    DB,24X,7HOVERALL )
  508 FORMAT( 6X,12HDEG     NOISE,11X,1H1,8X,1H2,8X,1H3,8X,1H4,8X,1H5,8X,
     * 1H6,8X,1H7,8X,1H8,8X,1H9,7X,2H10,9X,10HNOISE - DB )
  510 FORMAT( 6X,I3,4X,5HSHEAR,4X,10F9.2,7X,F9.2 )
  512 FORMAT( 14X,4HSELF,4X,10F9.2,7X,F9.2 )
  514 FORMAT( 13X,5HTOTAL,4X,10F9.2,7X,F9.2 / )
  516 FORMAT(/// 13X,36HOVERALL   POWER   CALCULATIONS   ... // )
  518 FORMAT( 32X,7HOVERALL,12X,8HINTEGRAL / 13X,5HNOISE,11X,
     * 13HPOWER - WATTS,11X,5HVALUE / )
  520 FORMAT( 13X,5HSHEAR,5X,2E20.8 )
  522 FORMAT( 13X,5H SELF,5X,2E20.8 )
  524 FORMAT( 13X,5HTOTAL,5X,E20.8 )
```

```
  530 FORMAT( 1H1 )
  532 FORMAT( //  5X,13HCONSTANTS ... // 5X,4HA = E13.7,3X,6HRHO =
     1 E13.7,3X,10HPARTIAL = E13.7,3X,8H    U = E13.7 )
  534 FORMAT( 5X,4HC = E13.7,3X,6H  R = E13.7,3X,10H      M = E13.7,
     1 3X,8HALPHA = E13.7 )
  536 FORMAT( 5X,4HW = E13.7,3X,6H  D = E13.7,3X,10H   BETA = E13.7,3X,
     1 8H    V = E13.7 // )
  538 FORMAT( 22X,10F9.0 / )
C
      END

        3200 FORTRAN DIAGNOSTIC RESULTS = FOR   NOISES


NULL STATEMENT NUMBERS
      132         126         120
```

```
                                        3200  FORTRAN     (2,2)              /  /
      FUNCTION ALOG10( X )
C
      IF( X .LE. 0. )  20,10
C
   10 TENLOGE = 0.43429448192
      ALOG10 = TENLOGE * ALOG(X)
      RETURN
C
   20 ALOG10 = 0.
      RETURN
C
      END

        3200 FORTRAN DIAGNOSTIC RESULTS - FOR   ALOG10


NO ERRORS
LOAD,56
RUN
```

CASE 3. MANGIAROTTY DATA D = 2.86 IN., M = 0.80 3/19/69

CONSTANTS ...

A = 1.1500000E-01 RHO = 2.4200000E-03 PARTIAL = 6.1600000E 03 U = 2.6400000E 02
C = 1.1000000E 03 R = 6.0000000E 00 M = 4.4000000E-01 ALPHA = 2.5000000E-01
W = 2.5000000E 02 D = 2.3800000E-01 BETA = 9.8347107E-04 V = 1.0588166E-01

THETA DEG	NOISE	OCTAVE BAND LEVEL NOISE - DB 1 250	2 500	3 1000	4 2000	5 4000	6 8000	7 16000	8 32000	9 64000	10 128000	OVERALL NOISE - DB
0	SHEAR	76.23	92.11	102.70	103.84	84.74	0	0	0	127.60	127.60	106.51
	SELF	70.47	84.93	97.67	104.49	97.97	53.55	0	0	127.60	127.60	106.08
	TOTAL	78.90	92.87	103.88	107.19	98.17	53.55	0	0	127.60	127.60	109.31
10	SHEAR	77.77	91.65	102.24	103.40	84.32	0	0	0	127.60	127.60	106.07
	SELF	70.21	84.67	97.41	104.24	97.73	53.36	0	0	127.60	127.60	105.83
	TOTAL	78.48	92.44	103.48	106.85	97.92	53.36	0	0	127.60	127.60	108.96
20	SHEAR	76.42	90.30	100.91	102.08	83.07	0	0	0	127.60	127.60	104.74
	SELF	69.47	83.93	96.67	103.52	97.04	52.79	0	0	127.60	127.60	105.11
	TOTAL	77.29	91.20	102.30	105.87	97.21	52.79	0	0	127.60	127.60	107.94
30	SHEAR	74.23	88.11	99.73	99.40	81.01	0	0	0	127.60	127.60	102.58
	SELF	66.30	82.76	95.51	102.39	95.95	51.88	0	0	127.60	127.60	103.98
	TOTAL	75.29	89.22	100.42	104.34	96.09	51.88	0	0	127.60	127.60	106.35
40	SHEAR	71.25	85.14	95.77	97.02	78.19	0	0	0	127.60	127.60	99.65
	SELF	66.81	81.27	94.03	100.93	94.55	50.68	0	0	127.60	127.60	102.53
	TOTAL	72.59	86.63	98.00	102.41	94.65	50.68	0	0	127.60	127.60	104.34
50	SHEAR	67.52	81.41	92.06	93.34	74.61	0	0	0	127.60	127.60	95.95
	SELF	65.10	79.57	92.34	99.26	92.93	49.26	0	0	127.60	127.60	100.87
	TOTAL	69.49	83.60	95.21	100.25	93.00	49.26	0	0	127.60	127.60	102.08
60	SHEAR	62.98	76.88	87.54	88.86	70.21	0	0	0	127.60	127.60	91.45
	SELF	63.28	77.75	90.53	97.47	91.19	47.70	0	0	127.60	127.60	99.08
	TOTAL	66.14	80.34	92.30	98.03	91.22	47.70	0	0	127.60	127.60	99.77
70	SHEAR	57.34	71.24	81.92	83.26	64.69	0	0	0	127.60	127.60	85.85
	SELF	61.43	75.90	88.68	95.65	89.41	46.07	0	0	127.60	127.60	97.26
	TOTAL	62.66	77.18	89.51	95.89	89.42	46.07	0	0	127.60	127.60	97.57
80	SHEAR	49.29	63.19	73.88	75.25	56.73	0	0	0	127.60	127.60	77.82
	SELF	59.61	74.08	86.87	93.86	87.65	44.44	0	0	127.60	127.60	95.47
	TOTAL	60.00	74.42	87.09	93.92	87.65	44.44	0	0	127.60	127.60	95.55
90	SHEAR	0	0	0	0	0	0	0	0	127.60	127.60	55.40
	SELF	57.89	72.36	85.15	92.15	85.97	42.86	0	0	127.60	127.60	93.77
	TOTAL	57.89	72.36	85.15	92.15	85.97	42.86	0	0	127.60	127.60	93.77

CASE 3. MANGIAROTTY DATA D = 2.86 IN., M = 0.80 3/19/69

THETA DEG	NOISE	OCTAVE BAND LEVEL NOISE - DB 1 (250)	2 (500)	3 (1000)	4 (2000)	5 (4000)	6 (8000)	7 (16000)	8 (32000)	9 (64000)	10 (128000)	OVERALL NOISE - DB
100	SHEAR	45,96	59,87	70,57	71,98	53,55	0	0	0	127,60	127,60	74,53
	SELF	56,29	70,76	83,56	90,57	84,41	41,38	0	0	127,60	127,60	92,19
	TOTAL	56,67	71,10	83,77	90,63	84,41	41,38	0	0	127,60	127,60	92,26
110	SHEAR	50,76	64,67	75,37	76,79	58,40	0	0	0	127,60	127,60	79,34
	SELF	54,54	69,32	82,12	89,14	82,99	40,03	0	0	127,60	127,60	90,76
	TOTAL	56,27	70,60	82,95	89,38	83,01	40,03	0	0	127,60	127,60	91,06
120	SHEAR	53,27	67,18	77,89	79,32	60,95	0	0	0	127,60	127,60	81,87
	SELF	53,57	68,04	80,85	87,87	81,74	38,83	0	0	127,60	127,60	89,50
	TOTAL	56,43	70,64	82,63	88,44	81,78	38,83	0	0	127,60	127,60	90,19
130	SHEAR	54,90	68,81	79,52	80,95	62,60	0	0	0	127,60	127,60	83,50
	SELF	52,48	66,95	79,76	86,79	80,67	37,80	0	0	127,60	127,60	89,41
	TOTAL	56,56	70,99	82,65	87,80	80,74	37,80	0	0	127,60	127,60	89,63
140	SHEAR	56,03	69,94	80,65	82,09	63,75	0	0	0	127,60	127,60	84,63
	SELF	51,58	66,06	78,86	85,90	79,78	36,94	0	0	127,60	127,60	87,52
	TOTAL	57,36	71,42	82,86	87,41	79,89	36,94	0	0	127,60	127,60	89,32
150	SHEAR	56,91	70,72	81,44	82,88	64,56	0	0	0	127,60	127,60	85,43
	SELF	50,58	65,35	78,16	85,20	79,09	36,27	0	0	127,60	127,60	86,82
	TOTAL	57,60	71,83	83,11	87,20	79,24	36,27	0	0	127,60	127,60	89,19
160	SHEAR	57,34	71,25	81,97	83,41	65,09	0	0	0	127,60	127,60	85,95
	SELF	50,37	64,85	77,66	84,70	78,59	35,78	0	0	127,60	127,60	86,32
	TOTAL	58,13	72,14	83,34	87,11	78,78	35,78	0	0	127,60	127,60	89,15
170	SHEAR	57,64	71,55	82,27	83,71	65,40	0	0	0	127,60	127,60	86,25
	SELF	50,07	64,55	77,35	84,40	78,29	35,49	0	0	127,60	127,60	86,02
	TOTAL	56,34	72,34	83,48	87,08	78,51	35,49	0	0	127,60	127,60	89,15
180	SHEAR	57,73	71,65	82,37	83,81	65,50	0	0	0	127,60	127,60	86,35
	SELF	49,97	64,45	77,25	84,30	78,19	35,40	0	0	127,60	127,60	85,92
	TOTAL	58,41	72,40	83,53	87,07	78,42	35,40	0	0	127,60	127,60	89,15

OVERALL POWER CALCULATIONS ...

NOISE	OVERALL POWER - WATTS	INTEGRAL VALUE
SHEAR	9.53237012E-01	4,95372730E 00
SELF	1.84391046E 00	5,29302279E 00
TOTAL	2.79714747E 00	